UNIVERSITÄT SIEGEN

Digital Video Stabilization of an Oscillating Camera using an Inertial Measurement Unit

Master Thesis

MS Mechatronics

Carl Zeiss AG, Jena,
Corporate Research Department (CRT)
and
Department of Mechatronics
Naturwissenschaftlich-Technische Fakultät
Universität Siegen

Ibad Rather (Matr. No. 1532894)

November 11, 2022

Supervisors:
Company: Dr. Steffen Urban
University: Prof. Dr. Ing. Bhaskar Choubey

Abstract

Video stabilization is ubiquitous in today's smartphones and action cameras. However, instead of classical "post-processing" image stabilization where image features are extracted and tracked over time [1] or modern deep learning based methods using dense optical flow [2], they need to perform the motion estimation on constrained hardware systems and with very high frame-rates ($\geq 120 fps$)

Hence the motion estimation, that is necessary to correct vibrations, shaking or rolling shutter distortions is performed using Inertial Measurement Units (IMUs). Typically, the motion estimates are reduced to rotational motions [3] (using gyroscopes) as the distance between frames is small and the field-of-view of the lenses large ($\geq 50°$). In addition, estimating translational motion is a difficult challenge using low-cost IMUs as the double integration of accelerometer readings is prone to strong drift and leads to large errors even over short time periods ($\leq 1s$).

This thesis should investigate and develop an image stabilization method for an oscillating camera. The camera has a small field-of-view and hence small translational movements along the viewing direction will be visible and need to be stabilized. The camera is coupled with an IMU and attached to a linear stage, that will mimic the oscillating movements. The camera records a monitor or a static target. An additional goal is the implementation, optimization and testing of the proposed algorithm on a modern embedded chip.

Contents

List of Tables

List of Figures

Chapter 1

Introduction

Cameras have become an integral part of our lives. We use cameras regularly, be it a smartphone camera, a hobbyist camera setup or professional cameras. Our demands for high quality media from cameras is also increasing constantly. We want sharper, color accurate, low lighting bright photographs. The videos are expected to capture scenes with as much realism as possible and we don't want too many movements in them irrespective of the way we capture them. If we are making a video capturing a beautiful sunrise or a landscape while walking, we do not want movements associated with walking in our video. We want it to be as smooth as possible. This is where *Image Stabilization* comes into play. Its goal being producing a stable video irrespective of the camera movements during capture. Stabilization is a very important quality metric for videos. A video may have all the aspects of photography correct but if it has too many sudden movements it would not look good.

1.1 Motivation

Image stabilization is a key technology to produce good quality photographs and videos. Be it a 250,000 Euros television broadcast camera or a 100 Euros hobbyist camera, stabilization of some sort is necessary. That is why image stabilization exists in every camera and smartphone these days. There even exists a series of product lines from many big companies like DJI just for this specific reason; to stabilize the image (video). These products can cost between 80 Euros for hobbyists to 1300 Euros or more for professionals. This clearly indicates that the need for stabilization is there and constant efforts are being put to make it better.

On microscopic level, the stabilization of videos becomes even more important as even small movements can cause large pixel shifts in the image plane. This can be seen by zooming in on your camera while trying to keep it stable. The effect of magnification becomes more evident and it will become

increasingly more difficult to keep the image smooth and stable as the movements are magnified as well. This happens because at a microscopic level the movements are also magnified. This will deteriorate the video quality and is very important to deal with.

Microscopic movements are the scope of this work. A modified GoPro Hero 10 (figure 1.1) camera is used as it allows to extract synchronized sensor and video data. The wide angle fisheye lens of the GoPro was exchanged with a narrow field-of-view lens that has a very large focal length. Switching the lens resulted in the default stabilization provided by GoPro (HyperSmooth) to not work anymore. The goal of this work is to explore different methods to obtain a stabilized video stream for large focal length lenses.

Figure 1.1: GoPro Hero 10

1.2 Challenges of the Work

For this work, an Inertial Measurement Unit (IMU) sensor will be used to stabilize the magnified video. This presents many challenges and requires the use of the state of the art neural network based techniques present today. Some of the challenges that were faced for this work and the requirements are as follows:

- Sensors are inherent to noise and this especially makes working with an IMU difficult because for position estimation we need to double integrate the signal. This double integration of the noisy signal causes a **drift** which is very undesirable for any image stabilization algorithm.
- Working with this drift is especially not possible in this case as we have a precision requirement of about 0.1 mm for the stabilization to work effectively.
- There exist IMU sensors with better noise characteristics, however, those are very expensive (in the order of 10k€) and it is difficult to buy them as they usually have a tactical grade placing them under export restrictions. Hence in this work a low-cost consumer MEMS IMU is used.

- IMUs have been used for position estimation for a long time using the classic Kalman Filter and its variants. They produce acceptable results for some cases but would not work in our cas[illegible]MUs are also generally coupled with cameras, GPS and Magnetometers to improve the precision but it is not possible for this use case.
- To overcome some of the challenges I am using neural networks. The use of neural networks creates challenges of data generation for training and testing. Neural network implementations for any task require a huge amount of data and the ground truth associated with it.
- Creating this data is very challenging and a lot of care needs to be taken about domain randomisation so the network generalizes well.

There are a lot of challenges in this work to overcome and that makes this exciting. In the next chapter of this report, I will discuss the fundamental of image stabilization and which methods are used.

Chapter 2

Fundamental Blocks of the Work

In the previous chapter I discussed the importance of Image Stabilization (Video Stabilization) and the challenges associated performing it using an IMU sensor. This chapter contains the image stabilization techniques available and also we make a case for our chosen technique. Then we will also discuss in depth the challenges associated with IMU pose-estimation and how we can overcome those challenges. Types of neural networks and their applications will also be briefly conferred as they are a huge part of this work.

2.1 Image Stabilization

If a camera is not stationary during video capture the output video quality may degrade and not look good. Depending on the movements during capture, video may look very shaky or even the subjects may not be properly visible. This is very undesirable and can cause visual discomfort (Jia and Evans, 2012). The solution to this may be to keep the camera steady by mounting it on stable tripod or to a rigid object. But this is not practically possible all the time. There are various scenarios in which the camera may move around a lot and the movements may not be smooth at all e.g an action camera mounted on a helmet or a bicycle, a camera mounted on a car or a robot in wild or some move-able rig or a robot arm.

The motion of the camera can be high-frequency tremors due to vibration, shaking or jiggling of the mounting point (Ryu and Chung, 2012) or low frequency such as movement of handheld camera during walking (Guilluy et al., 2021). Practically, in most of the video recording scenarios, the camera will have some movement. The goal of image stabilization is to create a output video with same visual content without the undesired movements.

2.1.1 Types of Image Stabilization

To deal with such movements and to make the video stable various techniques exist. These techniques are grouped in two categories:

- Hardware Image Stabilization
- Digital Image Stabilization

There are techniques which combine both these methods and are called Hybrid Image Stabilization techniques.

The goal of each of these stabilization techniques is to estimate the motion or pose and then use the estimated motion to stabilize the video. Motion/pose estimation will be discussed in the section 2.2 in detail.

Hardware Image Stabilization (HIS)

Hardware image stabilization at its core means moving the lens or the image sensor or the camera setup itself to counteract these movements while recording the video. The movements of camera can be minimised by the use of mechanical stabilizers like tripods or dollies (Grundmann et al., 2011). The use of electronic gimbals for video recording has also increased recently for both professionals and hobbyists. Video can also be stabilized by varying the optical path between lens and the image sensor. This is generally achieved by using electronic motors and IMU sensors to move around the lens or the image sensor or both to cancel out the motions. After the motions have been counter-acted upon, images are captured which results in a stabilized video output as seen in figure 2.1. These methods although mostly effective are not perfect and have both advantages and disadvantages.

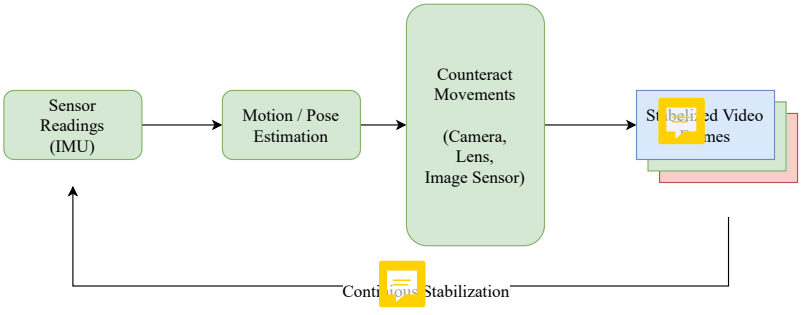

Figure 2.1: Hardware Image Stabilization

Advantages of HIS:

- No post-processing for stabilization needed.
- Works irrespective of the nature of object being captured.

- Full image without cropping can be used.
- Shutter Speed of the camera can be reduced

Disadvantages of HIS:

- Camera setups are very bulky.
- These solutions can be very expensive.
- More moving parts means higher maintenance.
- Cannot be improved once hardware is implemented.
- Not possible on all camera setups.

Digital Image Stabilization (DIS)

Digital Image Stabilization also called Digital Video Stabilization (DVS) is a software based image stabilization technique (Guilluy et al., 2021). The technique here is similar what is done is HIS i.e. first motion of the camera is estimated (pose-estimation) and based on this, the image is stabilized. The difference here is that after pose estimation is done, instead of moving around the hardware a suitable transformation (warping) is applied to the image (Censi et al., 1999) as shown is figure 2.2. The resulting stabilized image (video) is motionless irrespective of the camera motions. DIS is be a very powerful technique but like other methods and techniques, it has its advantages and disadvantages.

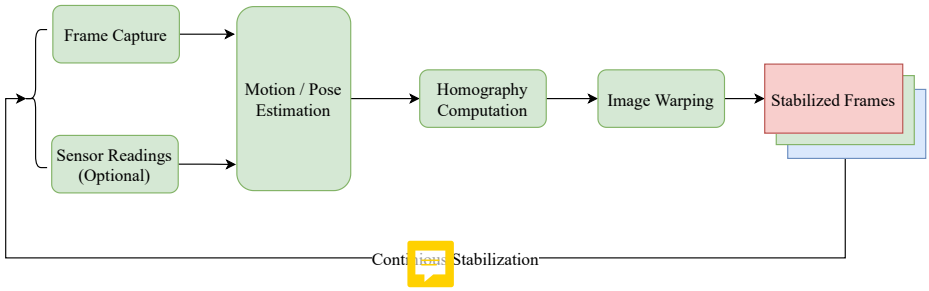

Figure 2.2: Digital Image Stabilization

Advantages of DIS:

- Cost effective.
- Smaller camera setups can be used.
- No necessary changes need to be made to the camera setup for DIS.

- Can be achieved using IMU sensors for pose estimation which are not very expensive.
- Can be applied to any video; even the historic ones.
- Different DIS algorithms can be used on a single video in post processing.
- Relatively easy to modify DIS software.

Disadvantages of DIS:

- The resolution of the output images (video) is reduced (generally by 5 to 10 percent).
- May require some manual labour (like in Adobe Premiere Pro: manual feature tracking).
- Some videos are very difficult (even impossible) to stabilize if there is too much vibration or the features are not visible.
- May require a lot of computational power (optical flow)

Now we know that for any type of image stabilization motion estimation is fundamental and this is what will be discussed in the next section of this report.

2.2 Motion Estimation for Image Stabilization

Camera motion (pose) estimation is very important and one of the most challenging parts of image stabilization. Before hardware and digital stabilization techniques/algorithms can be implemented, we need to perform pose estimation to figure out the camera motions. Then based on these camera motions we can stabilize a video. The accuracy of motion estimation ultimately determines the effectiveness of image stabilization (Ryu and Chung, 2012). To estimate the camera motion many sensor based and software based techniques exist as show in figure 2.3.

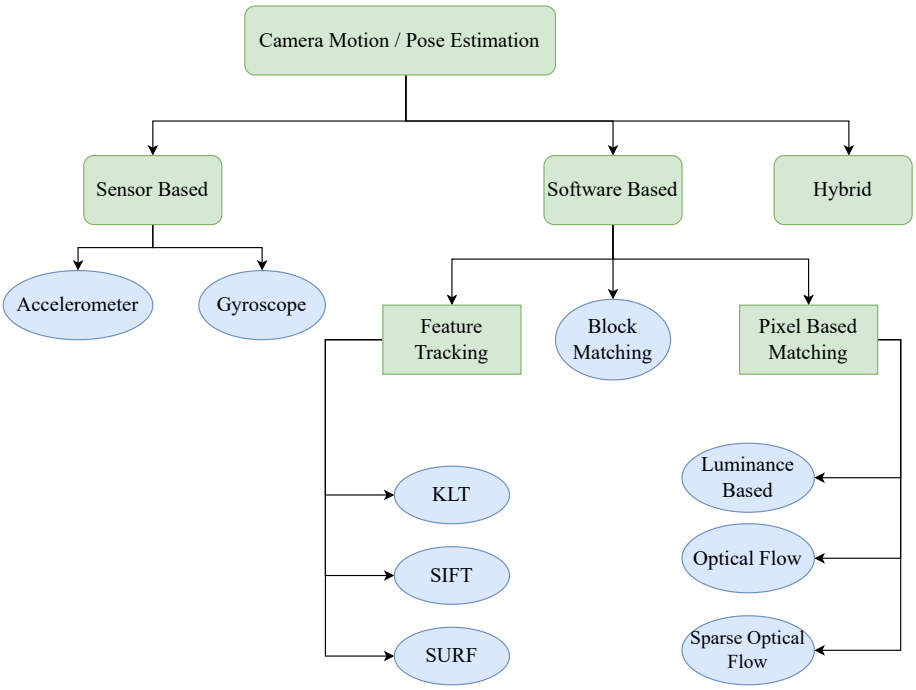

Figure 2.3: Camera Motion/Pose Estimation Techniques

2.2.1 Software based motion estimation techniques

Software based motion estimation techniques/algorithms use the images (frames) coming from the camera for motion estimation and subsequently for stabilization. Some of these software based techniques are listed below (Guilluy et al., 2021):

- Pixel-based matching
- Block-Matching
- Feature-Matching

Each of these approaches/algorithms used in motion estimation are briefly discussed in the subsequent sections. This will also lay a foundation for why we are not using any of these techniques for this work.

Pixel-Based Matching

This method estimates pose by determining the motion of pixels between two frames (Guilluy et al., 2021). For correspondence determination, luminance of two consecutive frames is assumed to be constant throughout. This poses a problem and there can be many pixels having same luminance, so, other constraints are also needed to obtain a unique solution (Guilluy et al., 2021).

Finding ***Optical Flow*** between two consecutive frame is another method for motion estimation. Optical flow is the distribution of apparent velocities of movement of brightness patterns in an image (Horn and Schunck, 1981). This gives us important information about the spatial arrangement of the objects viewed and the rate of change of this arrangement (Gibson, 1977). Using this information, relative motions can be estimated between consecutive image frames. These relative motions can be used for camera motion estimation. Many modern neural network based optical flow algorithms have also been developed recently and are used in image stabilization tasks (Shi et al., 2022). Although this method can give us good results, but, it has very high computational requirements and thus can be very slow.

Block-Matching

Block matching techniques use blocks of pixels for motion estimation instead of finding correspondence between pixels of consecutive frames. This allows to remove some ambiguities that occur in pixel-based matching methods (Guilluy et al., 2021). Block-matching approach offers a flexible trade-off between complexity, computational efficiency and accuracy (Guilluy et al., 2021) but relies heavily on unambiguous features in the image.

Feature-Matching (Tracking)

In these methods, the algorithm first selects the features that are easily recognisable and distinguishable. The motion is estimated by tracking only these features, so it is make them computationally less expensive. There are several feature tracking algorithms that are widely used in many computer vision applications.

Kanade Lucas Tomasi (KLT) feature tracker (Tomasi and Kanade, 1991) is a widely used feature tracking algorithm in computer vision. Features are selected and their position is initialized using this technique and then optical flow is used to track their position (Guilluy et al., 2021).

Scale-invariant feature transform (SIFT) is also used for motion estimation in digital image stabilization algorithms. It has been designed for extracting highly distinctive invariant features from images, which can be used to perform reliable matching of the same object or scene between different images (Battiato et al., 2007). It contains the orientation of the feature in order to be rotation-invariant (Guilluy et al., 2021).

Speeded up robust features (SURF) is inspired by SIFT but is faster (Zheng et al., 2015). This technique is also widely used in feature selection and tracking for motion estimation.

A common theme here in software based motion estimation techniques is to detect features (be it a pixel, or a group of pixels or any other particular image feature) and then tracking it for motion estimation. But, there are certain use cases like ours where feature tracking is very difficult or unreliable. The features in an image sequence can be moving in different directions, which makes reliable motion estimation using these techniques impossible. This is the case for this work and the goal is to *estimate motion using technique which is image invariant*. To achieve this we decided to use sensor based pose-estimation techniques.

2.2.2 Sensor based Motion Estimation

Pose estimation is a huge area of research especially for the field of robotics and autonomous driving. There are various sensors like Accelerometers, Gyroscopes, Magnetometers and Satellite Navigation systems available. For camera pose estimation, generally Gyroscopes and Accelerometers are used. In combination, these two sensors are called *Inertial Measure Unit (IMU) Sensors*. For this work, we will be using IMU for pose estimation as using it has many advantages and will make our image stabilization algorithm image invariant.

2.3 Inertial Measurement Unit (IMU) Sensors

IMU sensor is one of the most commonly used sensors in the world and present all around us in mobile devices, virtual reality gear and cameras. It is very common to use IMU sensor for pose estimation. An IMU sensor measures acceleration(m/s^2) and angular velocity (rad/s). They can make these measurements in multiple degrees of freedom e.g., a 6-DoF IMU sensor includes a 3-axis accelerometer (x, y, z) and 3 axis gyroscope (x, y, z) (Constant et al., 2021). The accelerometer will make independent acceleration measurements in these axis. Similarly, the gyroscope makes independent angular velocity measurements about these three axis.

IMU sensors are used in a wide variety of applications like navigation, robotics, drones, smartwatches, sports learning, augmented reality systems, industrial quality control (Ahmad et al., 2013) and also for image stabilization in cameras. In all these applications, IMU sensor is used for pose estimation in some form; either for absolute pose estimation or change in pose.

There are a lot of reasons to use IMU sensors and these reasons are surely a very huge contributor to them being one of the most commonly used sensors in the world. Some of their qualities are (Woodman, 2007).:

- They have small size

- low weight
- rugged construction
- low power consumption
- cheap
- high reliability
- low maintenance
- can be used in hostile environments

2.3.1 Pose Estimation with IMUs

Pose for any object is its position(x, y, z) and its orientation(yaw, pitch, roll) with respect to some reference coordinate system. To estimate pose of an object, we continuously take measurements from IMU and using some algorithm we estimate its pose. Figure 2.4 below shows the strap-down inertial navigation algorithm (Woodman, 2007). For orientation estimation gyroscope readings are used and for position estimation both gyroscope and accelerometer readings are used. The use of this algorithm directly for pose-estimation is not possible as the IMU readings are far from being ideal, they contain noise and have a bias (Woodman, 2007) which needs to be accounted for.

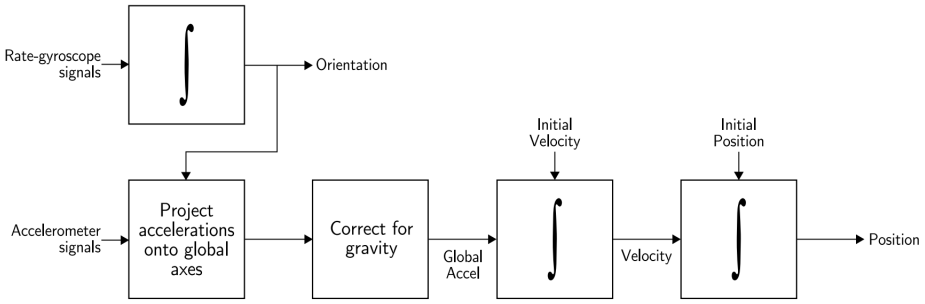

Figure 2.4: Strap-down inertial navigation algorithm (Woodman, 2007)

2.3.2 IMU Noise Models

MEMS sensor outputs are inherent to noise and there is different types of noise with which we have to deal. For IMUs, the readings coming from a sensor could be modelled as a combination of three entities: true signal, bias and white noise.

Gyroscope

$$\omega_n(t) = \omega(t) + b_g(t) + n_g \tag{2.1}$$

Where $\omega_n(t)$ is the noisy gyroscope signal, $\omega(t)$ is the true gyroscope signal, $b_g(t)$ is the gyroscope bias and n_g is the gyroscope white noise.

Accelerometer

$$a_n(t) = a(t) + b_a(t) + n_a \tag{2.2}$$

Where $a_n(t)$ is the noisy accelerometer signal, $a(t)$ is the true accelerometer signal, $b_a(t)$ is the accelerometer bias and n_a is the accelerometer white noise.

To visualise the *Noise Model*, let's take a true unit signal as show in figure 2.5. **Bias** can be defined as constant offset from true signal value. White noise can be thought of as random fluctuations of equal intensity and different frequency from the true value of the signal (2.5).

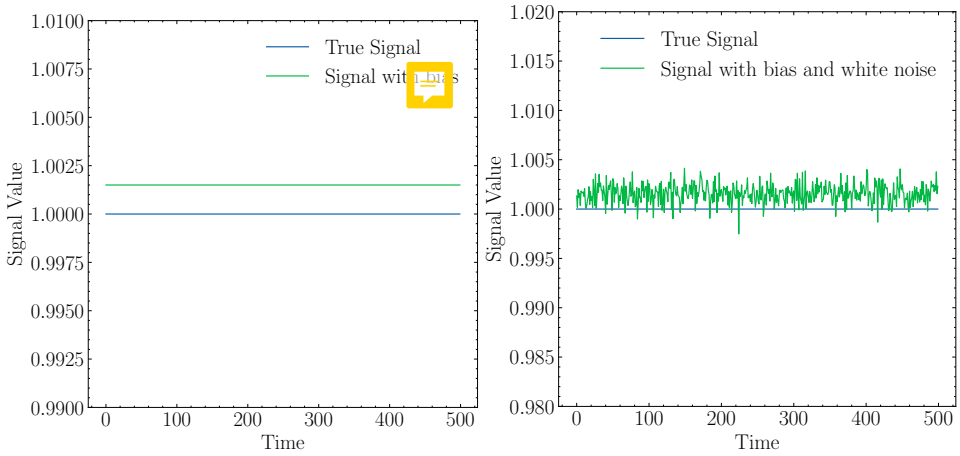

Figure 2.5: IMU Noise Model Visualisation

For both gyroscope and accelerometer the signal can be independently modeled this way in each of its axis (x, y and z) (Trawny and Roumeliotis, 2005). As you can see from the plots, the noisy signal looks very different from the true signal. Using the noisy signal directly for pose estimation can lead to very inaccurate results. Although the modelling equation looks the same for both gyroscope and accelerometer, but they have different effects on pose estimation as the strap-down inertial algorithm suggests. So, there are different challenges associated with position and orientation estimation using this sensor with absolute position estimation being especially h

Gyro Error Characteristics

To get orientation from the gyroscope, the readings need to be integrated once and the global orientation needs to be updated. This needs to be done for each of the gyroscope axis. Doing this continuously with the noisy signal will result in erroneous orientation tracking if nothing is done about the

noise. In table 2.1 you can see all the errors and effect of those on orientation measurement.

Accelerometer Error Characteristics

Generating position information from accelerometer is not a single step like in case of Gyroscope. Based the strap-down inertial navigation algorithm shown in figure 2.4 there are multiple steps involved. First, the accelerometer readings need to be projected into the global axis using the orientation calculated from gyroscope. Then, the accelerometer reading needs to be corrected for gravity. After that we double integrate the signal based on initial velocity and initial position to finally get the position.

So, there is double integration present in the algorithm. We also have a noisy signal, so, the noise also gets integrated two times. This can result into very inaccurate position estimations and is one of the most challenging parts of working with an IMU. In table 2.1 you can see all errors in an MEMS accelerometer and effect of those on position measurement.

Error Type	Description	Result of Single/Double Integration
Accel Bias	A constant Bias ϵ	Steadily growing angular error. $\theta(t) = \epsilon(t)$
Accel White Noise	White noise with some standard deviation σ	An angular random walk, whose standard deviation grows with the square root of time. $\sigma_\theta(t) = \sigma\sqrt{\delta t}$
Gyro Bias	A constant Bias ϵ in the accelerometer's output signal.	A quadratically growing position error. $s(t) = \epsilon\frac{t^2}{2}$
Gyro White Noise	White noise with some standard deviation σ	A second order random walk. The standard deviation of the position error grows as $\sigma_s(t) = \sigma t^{\frac{3}{2}}\sqrt{\frac{\sigma t}{3}}$

Table 2.1: Summary of IMU Error Sources (Woodman, 2007)

Challenges in Working with IMU

For the reasons mentioned in the previous sections, it is not straightforward to work with IMUs, especially for absolute position estimation as the errors introduced are squared with time. This results in a **drift** from actual position, which for any image stabilization algorithm is very detrimental. Orientation estimation is still relatively reliable and is the main reason why Gyroscope based hardware as well as digital image stabilization is more common.

2.4 Pose Estimation using IMU

Based on the strap-down inertial navigation algorithm (Section 2.4) and Newtonian mechanics, pose can be estimated from the IMU readings using equation 2.3 and equation 2.4. We need a history of pose for the iterative pose estimation to work. ω and a are the gyroscope and accelerometer readings respectively as defined in section 2.3.

$$[H]O(t) = O(t - dt)exp(\int_{t-dt}^{t} \Omega(t)dt) \tag{2.3}$$

Orientation $O(t)$ is the updated orientation in global frame at current timestamp using orientation at previous timestamp $O(t-dt)$ and the sensor readings $\Omega(t)$ as shown in equation 2.3.

$$\begin{aligned} a_g(t) &= O(t).a(t) \\ [H]v(t) &= v(t - dt) + (a_g(t) - g_g).dt \\ P(t) &= P(t - dt) + v(t).dt \end{aligned} \tag{2.4}$$

Position estimation can be done using a series of mathematical equations as shown in equation 2.4. The accelerometer readings are first projected onto the global axis based on the orientation $O(t)$. Then the current velocity $v(t)$ is calculated by integrating the acceleration $a_g(t)$ and adding it to velocity at previous time-step $v(t - dt)$. Finally, to get the current position $P(t)$ we integrate the velocity $v(t)$ add it to the previous position.

These equations are the backbone for classical pose estimation algorithms using IMU sensors. Bias and white noise present in the sensor readings also integrates causing a **drift** in estimation. In case of Gyroscopes, white noise causes an *angular random walk* whose standard deviation grows proportionally with square root of time (Woodman, 2007). And leaving the bias unchecked for causes an orientation error growing linearly with time as shown in table 2.1. In case of accelerometer the drift is aggravated because the orientation error is also contributing to it. The subtraction of gravity g from the readings is not perfect either and causes further drift. The bias in the readings also increases the error (hence the drift) quadratically with

time. On top of all these errors the effect of white noise is a *second order random walk* whose standard deviation increases quadratically with time as shown in table 2.1.

We can very comfortably conclude that using the inertial navigation system in its pure form is not possible for accurate pose estimation. There are several techniques which can be used to diminish the effect of the noise and the bias. Bias can be estimated for any IMU sensor by keeping it stationary for a few seconds. The readings that we get for a stationary IMU sensor is the bias for that sensor. Then this bias can be adjusted in the signal recorded during operation.

But modern learning based methods do not use these equations. Instead they are more data driven and let the neural network infer these relations based on the training data.

2.4.1 Classical Techniques

IMUs have been used extensively for pose estimation for the better half of the century and were used to track the Apollo 11 rocket that took man to the mars. Over the years many techniques and algorithms have been developed to improve pose-estimation accuracy using IMU. These techniques range from simple signal filtering to more advanced state-estimation algorithms.

Signal Filtering

There are also various signal-processing techniques that can be used to reduce the white noise. Noise can be characterised as a high-frequency content in any signal. Therefore, we can use simple filters like a low pass filter or a moving average filter with big horizon to eliminate the noise up to some extent. These techniques are in no way perfect and may even cause loss of true signal if not configured properly.

Kalman Filter

Kalman filters are very useful for estimation purposes. They can be used to estimate pose using an IMU sensor by filtering noise based on a covariance matrix (Ferdinando et al., 2012). The values of this covariance matrix can be varied but there is a trade-off between noise sensitivity and accuracy. Kalman filter is used to fuse multiple sensors to improve the accuracy of estimation. But in our case the accuracy it provides over time is not enough ((Kok et al., 2017), (Alatise and Hancke, 2017), (Bangera et al., 2020)) and hence cannot be used.

These techniques may be good enough for some other applications, but in our case their use is not enough. The precision requirements are very high. Even with the use of these algorithms, there is still a drift present which is unacceptable for this use case.

2.4.2 Neural Network Based

With the advancement of neural networks and their ability to outperform classical algorithms over the years many techniques have been developed to solve the challenge of double integrating accelerometer readings. Based on the fact that the vibrations in our camera setup have similar characteristics and patterns, a neural network can learn that pattern and make accurate predictions. Some of the techniques which laid the foundation of the methodology we used are discussed in chapter 3 of this report.

2.5 Neural Network Architectures

The evolution of neural networks and deep learning techniques over the past decade has made the use data driven approaches very common in overcoming challenges. Data driven approaches have surpassed classical techniques in many applications. There are various neural network architectures, their variations and combinations present today. Each of these architectures have properties that aid in achieving solutions for various challenges.

2.5.1 Multi Layer Perceptron (MLP)

MLPs are the simplest form of Artificial Neural Networks (ANNs) or Deep Neural Networks (DNNs) and are made of a combination of perceptrons/ neurons (figure 2.6). An MLP has at-least three layers; an input-layer, a hidden layer and an output-layer as shown in figure 2.7. The network learns by changing weights of its layers with the forward and backward pass using some optimization algorithm (gradient descent). These networks act as universal function approximators (Cybenko, 1989) and therefore are used to create mathematical models by regression analysis. We will be using MLPs as Fully Connected (FC) layers in all of our networks for this purpose.

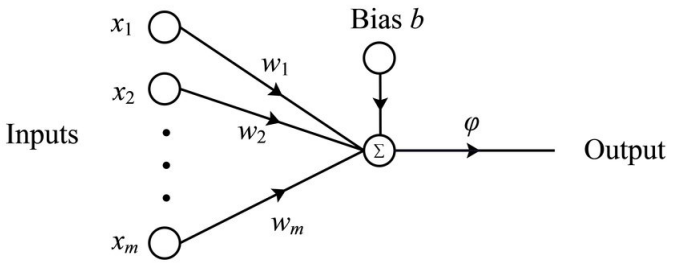

Figure 2.6: Perceptron

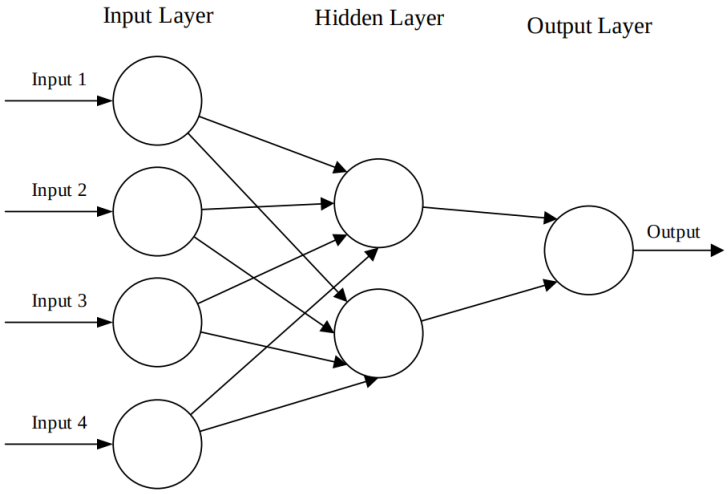

Figure 2.7: Multi Layer Perceptron

2.5.2 Convolutional Neural Networks (CNNs)

CNNs are another class of ANNs and are responsible for revolutionising the field computer vision and has applications in Natural Language Processing, Recommender Engines and Time Series. These networks also have neurons that self-optimise through learning (O'Shea and Nash, 2015). These networks are capable of learning multiple features from the data by abstracting the data into feature maps. In our case we input a 6 channel (3-accelerometer and 3-gyroscope) data and then the CNNs take the data from 6 channels to 64 channels (feature maps). Then these features are fed into the Fully Connected Layers (FC / MLP) at the end to regress the pose as shown in figure 2.8. This also results in reducing dimensionality of the data while regressing the output.

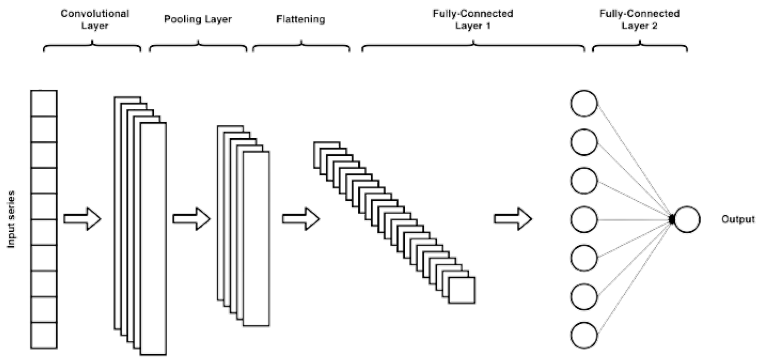

Figure 2.8: CNN layers with FC layers

2.5.3 Transformers

Transformer architecture as shown in figure 2.9 is one of the latest proposed neural network architectures that has outperformed its predecessors. Its use mainly started for natural language processing (Vaswani et al., 2017) but was also adopted for computer vision (Dosovitskiy et al., 2020). The use of transformers is also extended for Inertial based Human Activity Recognition (HAR) Shavit and Klein (2021) and Inertial Navigation (Rao et al., 2022). This architecture adopts Multi Headed Attention Mechanism (MHA) (Vaswani et al., 2017) which results in weighing the significance of each part of input data. This significantly improves performance of the network as it learns the importance of each feature and can look at the bigger picture from the data.

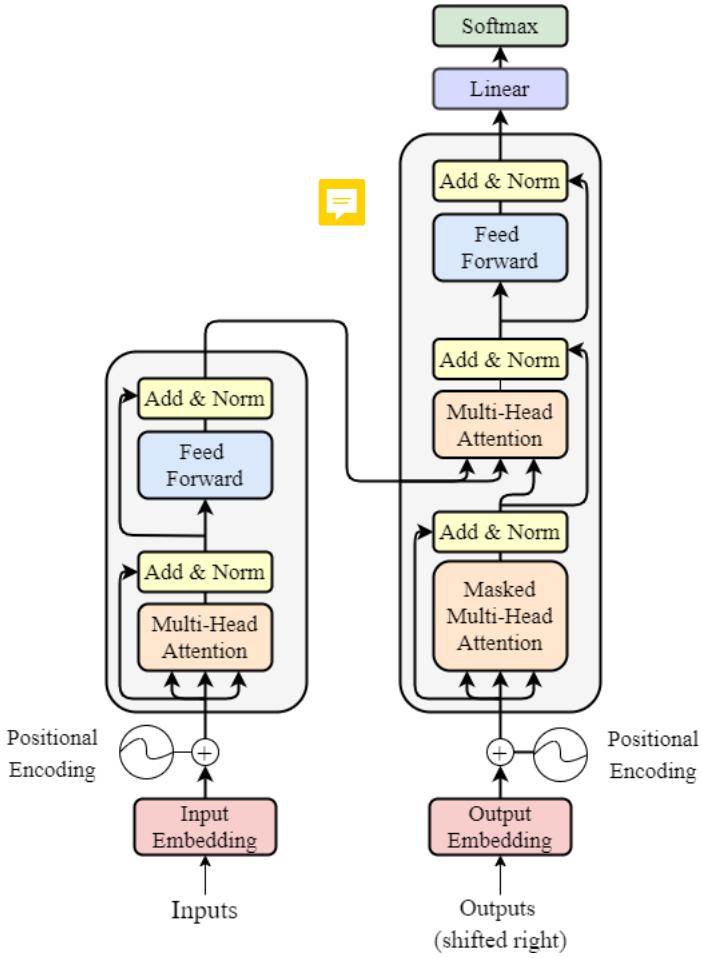

Figure 2.9: Transformer Architecture

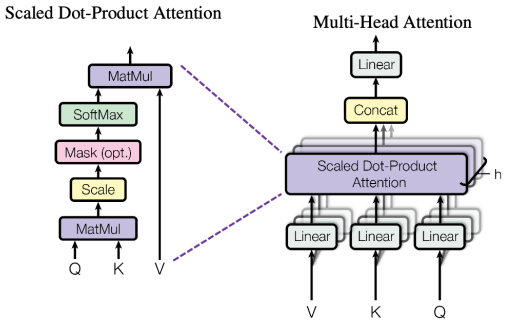

Figure 2.10: Multi Headed Attention

In this chapter we discussed different methods for image stabilization, challenges of pose-estimation and which methods are available to estimate pose from MEMS IMUs. The next chapter summaries some state of the art techniques used to solve the challenges we are facing.

Chapter 3

State of Research

Previous chapter laid out the foundations for image stabilization and motion estimation. We also made the case for the techniques and algorithms chosen for this work. Now, this chapter includes some of the state-of-the-art methods for digital image stabilization and pose estimation.

3.1 Digital Image Stabilization

Various sensor based digital image stabilization techniques have been developed over the years using both classical and data-driven approaches. These techniques are limited to rotational motion compensation or using image data.

3.1.1 5D Video Stabilization through Sensor Vision Fusion

This research aims to overcome the challenge of going beyond 3D stabilization (rotation only) by also including translational motion in their image stabilization algorithm for smartphones. The proposed 5D stabilization is achieved by carefully combining sensor based 3D rotation stabilization and vision based 2D translation stabilization (Zhuang et al., 2019). Figure 3.1 shows the block diagram for this approach. This method is promising as it deals with translational motion as well but does so using image features and hence cannot be used for our use case.

3.1.2 Deep Online Fused Video Stabilization

This work aims at stabilizing videos using *Gyroscope* data as well as *Optical Flow* through unsupervised learned (Shi et al., 2022). Instead of pose estimation, warping grid calculation and image warping the aim here is to directly warp the image based input data (images and gyroscope data) as shown in figure 3.2. The results seem to outperform some of the previous state-of-the-art methods present before it. Although very promising this

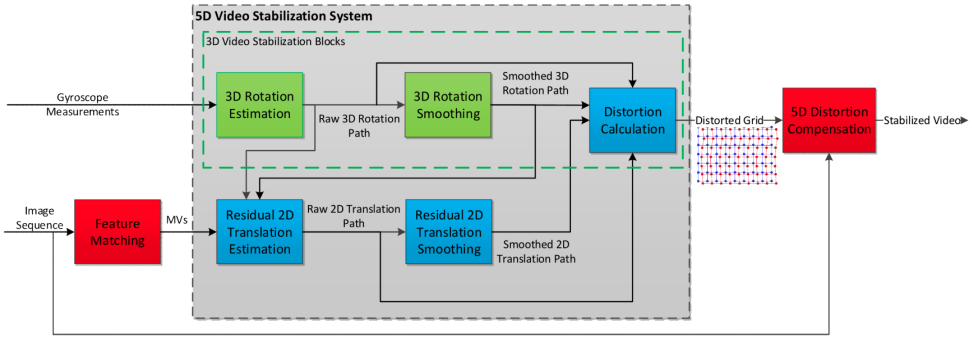

Figure 3.1: Block diagram for proposed 5D video stabilization system (Zhuang et al., 2019)

method cannot be used in our case as we want our algorithm to be image invariant based on reasons discussed in section 2.2.1. It also has a component of finding optical flow for each frame using a different neural network which makes this algorithm very computationally expensive and hence not usable all computers/hardware.

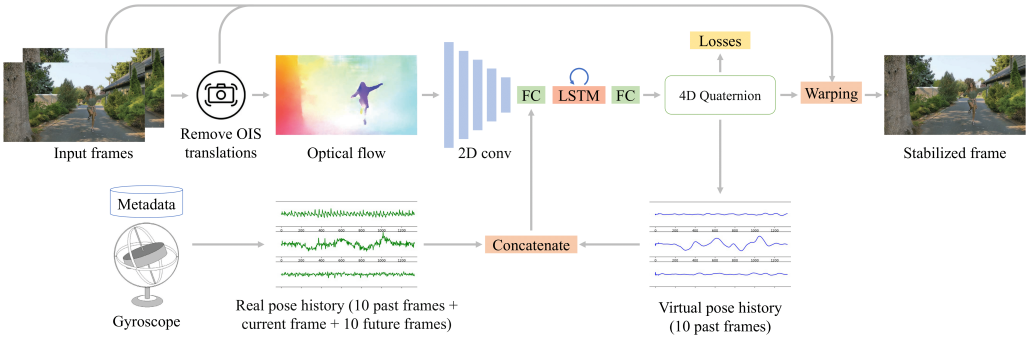

Figure 3.2: Deep online fused video stabilization overview (Shi et al., 2022)

3.2 Pose Estimation

Classical algorithms fail to accurately estimate the pose using MEMS IMU over a long period of time. With the advancement of artificial neural networks (ANNs) and their architectures new data driven techniques have been developed for this purpose. These data-driven techniques have f outperformed their classical predecessors and are becoming a standard for this purpose. But with al ese benefits they are computationally very expensive and have very high edge hardware requirements.

3.2.1 RIDI: Robust IMU Double Integration

RIDI was the first data-driven neural network approach which tackles the challenges of double integrating accelerometer readings. The algorithm regresses a velocity vector from the history of linear accelerations and angular velocities (IMU windows - discussed in section 4.2), then corrects low-frequency bias in the linear accelerations, which are integrated twice to estimate position (Yan et al., 2018). The analysis of results manifested that this algorithm outperformed the heuristic-based methods and even came closer to visual inertial navigation (Yan et al., 2018). The issue with this is it can only regress position and orientation estimation needs to be achieved using classical algorithms.

3.2.2 RoNIN: Robust Neural Inertial Navigation in the Wild

Developed by the same team as RIDI, RoNIN uses more advanced neural network architectures like ResNet, LSTM and TCN as its backbone to regress a velocity vecotor given a window of IMU samples (Herath et al., 2020). Input to the network in this case are the angular rates (Gyroscope readings), accelerations (accelerometer readings) and device orientations as shown in figure 3.3 and the output is motion trajectory (poses). Using these architectures and increasing the quality and size of data RoNIN outperforms RIDI and sets a new benchmark for inertial navigation (Herath et al., 2020). Our methodology is highly influenced by this technique and is discussed in chapter 4 of this report.

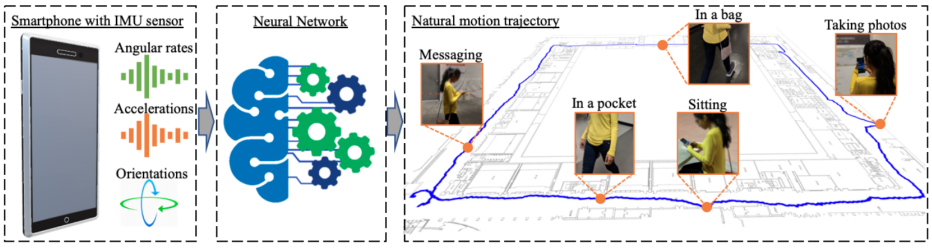

Figure 3.3: RoNIN process layout (Herath et al., 2020)

3.2.3 TLIO: Tightly Learned Inertial Odometry

This combines both classical and learn-based approaches by using an Extended Kalman Filter (EKF) and deep neural network (DNN). EKF is responsible for prediction step while outputs (displacement and uncertainty) from the neural network is used as measurement update. The filter estimates rotation, velocity, position and IMU biases at IMU rate (Hol et al., 2009) as shown in figure 3.4. We could not reproduce similar results as the research claimed using our datasets.

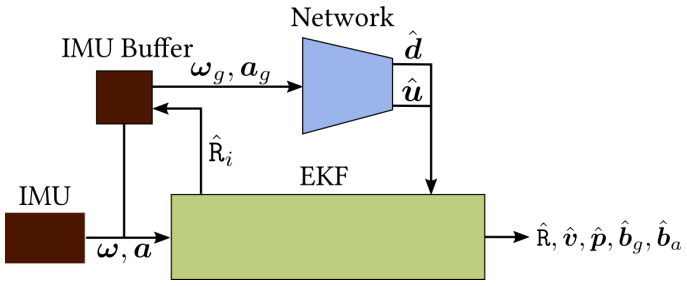

Figure 3.4: TLIO architecture (Hol et al., 2009)

3.2.4 CTIN: Robust Contextual Transformer Network for Inertial Navigation

This algorithm takes advantage of the recent advances in deep learning by using Multi-Headed-Attention (MHA) mechanism introduced in (Vaswani et al., 2017). It uses a ResNet based encoder enhanced by local and global MHA to capture spatial contextual information from IMU measurements (Rao et al., 2022) as shown in figure 3.5. CTIN is claimed to be robust and to outperform state-of-the-art models but cannot be evaluated as it is not available publicly.

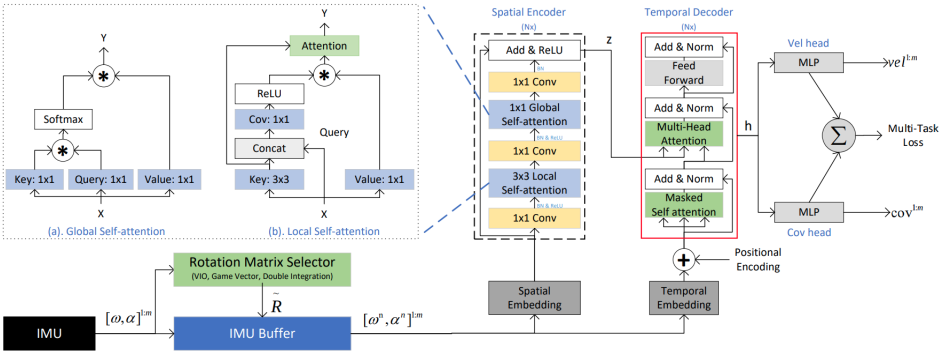

Figure 3.5: CTIN Architecture (Rao et al., 2022)

Chapter 4

Work Methodology

So far we have discussed the problem we are trying to solve, what are the methods available to us and the challenges associated with them. This chapter contains the process we used to digitally stabilize video for our use-case. Figure 4.1 shows the pipeline we are using to digitally stabilize videos in our case.

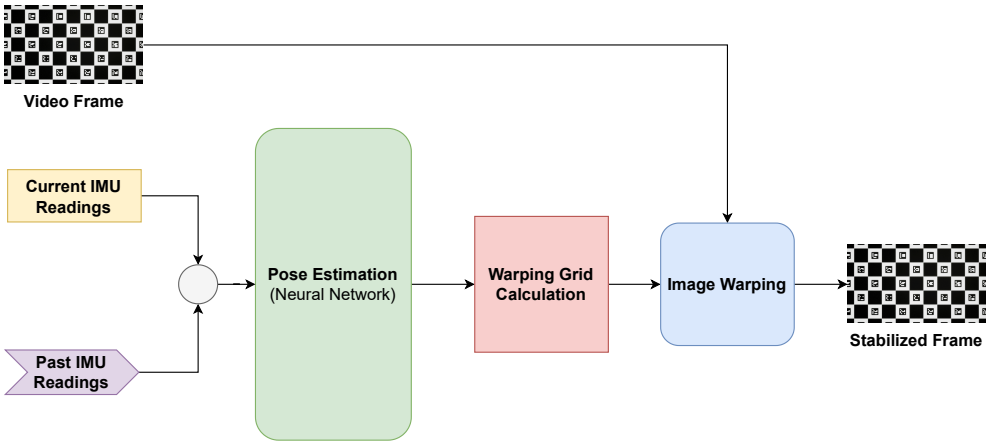

Figure 4.1: DIS pipeline using IMU Sensor

We will be using an IMU sensor for camera pose estimation to stabilize the video for this work. Based on the precision requirements of the pose-estimation algorithm we will be using a data-driven approach as classical signal processing and sensor fusion algorithms fail to provide this precision over a long period of time. For our data driven approach we build datasets using a camera and also simulation. To capture the video we are using a GoPro Hero 10 which provides synchronised image and sensor data capture. We also swapped the factory lens to a low Field of View (FOV) and high focal length lens (figure 4.2). The simulation was build using Unreal Engine

4 and Microsoft AirSim. Table 4.1 shows the technical specifications of the camera setup. For simulation similar camera parameters were used.

Image Sensor	Sony	Diagonal 7.85 mm (Type 1/2.3) 23.91 M CMOS Image Sensor with Square Pixel.
IMU Sensor	Bosch	6-axis IMU Sensor Accelerometer (A): 16-bit or 0.06 mg/LSB Gyroscope (G): 16-bit or 0.004 dps/LSB
Lens	xx	15° FOV and 200 mm focal length

Table 4.1: Hardware technical specifications

Figure 4.2: Modified GoPro Hero 10 with Low FOV and High Focal length lens

Figure 4.3: Bosch BMI260 IMU Sensor

4.1 Data Collection

Collecting data for any data driven approach is a challenging and an iterative process. The data or training data in this case are the readings coming from the IMU sensor and the target (ground truth) being the camera pose (position and orientation). Real data was collected by mounting the camera on a rig which had vibrations associated with it on movement (figure 4.4). We made sure that the data depicts real life scenarios by moving the rig around in many different ways and let it vibrate and collect the data. The ground truth was generated using proprietary Zeiss software and is beyond the scope of this work.

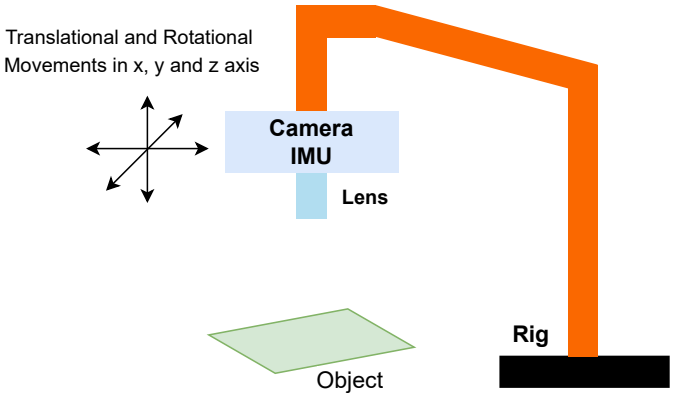

Figure 4.4: Camera rig setup

Then the data was collected from simulation based on the analysed real data and pushed beyond real data limits to account for even more challenging scenarios. Generating simulated data with accurate ground truth is a fast processes not requiring much post-processing. This also allowed us to tinker with noise and bias to make the neural network robust and generalize well.

4.1.1 Data Analysis

The data recorded from a camera-rig setup was analysed to determine the vibration and sensor parameters. Table 4.2 summarises the white noise and bias characteristics determined from the raw IMU Sensor Readings. These match closely with the data provided by the manufacturer. Accelerometer variance from data sheet $160\mu g/\sqrt{Hz}$ and for gyroscope $0.008dps/\sqrt{Hz}$.

Parameter	Value
Accelerometer Bias	xx
Accelerometer White Noise	$\mu = 0$ and $\sigma^2 = 0.00038 m/s^2$
Gyro Bias	xx
Gyro White Noise	$\mu = 0$ and $\sigma^2 = 0.xxx$

Table 4.2: IMU Noise Characteristics

We analysed the generated ground truth to determine the characteristics of vibration. These characteristics are important to understand the nature of vibration and to set the working limits for our work. Vibrations are characterised by **Amplitude** (A or θ), **Time Constant** (τ) and **Frequency** (ω). We have damped oscillations for both displacement and rotation vibration as shown in figure 4.5 and can be characterised by the equations 4.1 and 4.2.

$$A(t) = Ae^{-t/\tau} sin(2\pi\omega t) \tag{4.1}$$

$$\theta(t) = \theta e^{-t/\tau} sin(2\pi\omega t) \tag{4.2}$$

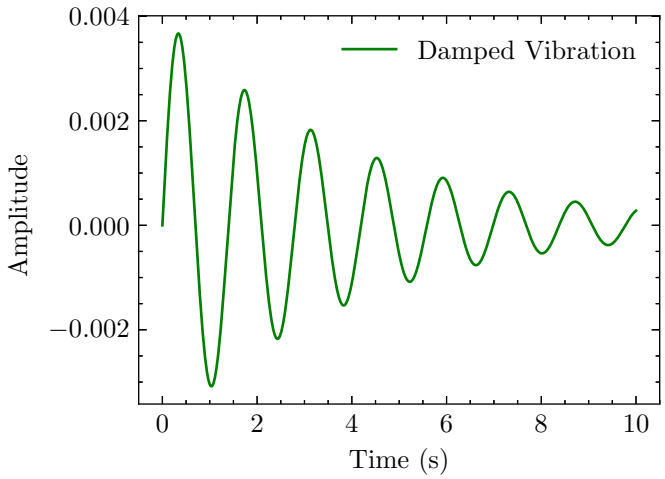

Figure 4.5: Damped Vibration

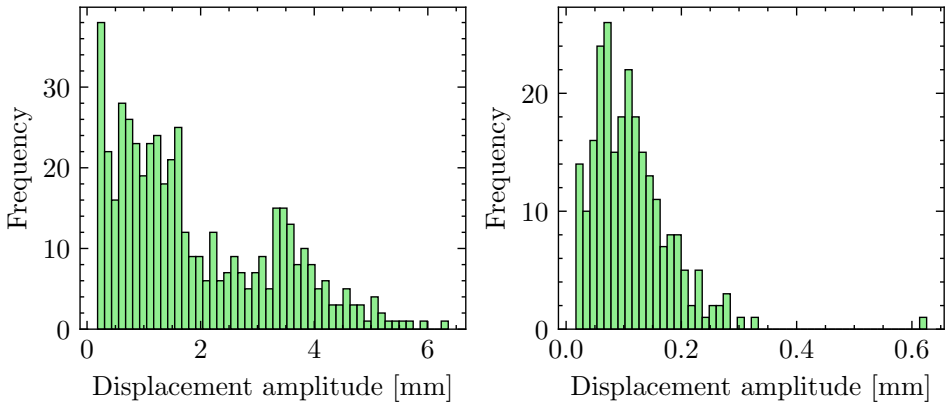

(a) Distribution of displacement amplitude A in XY(left) and Z(right) DoF [mm]

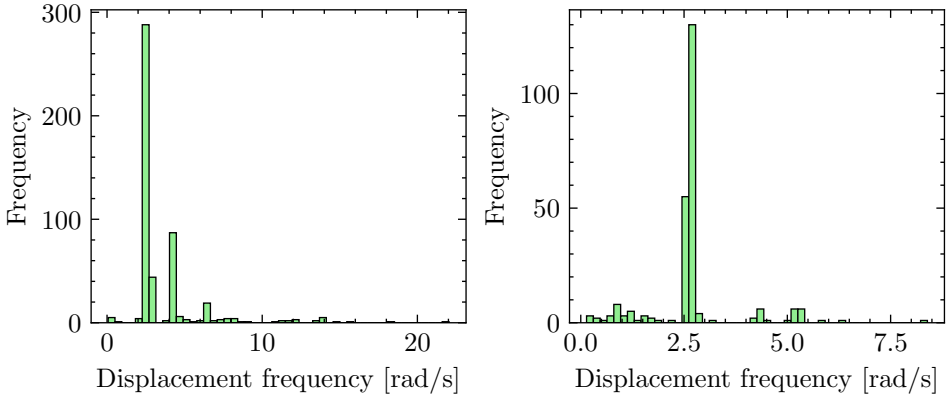

(b) Distribution of displacement frequency ω in XY(left) and Z(right) DoF [mm]

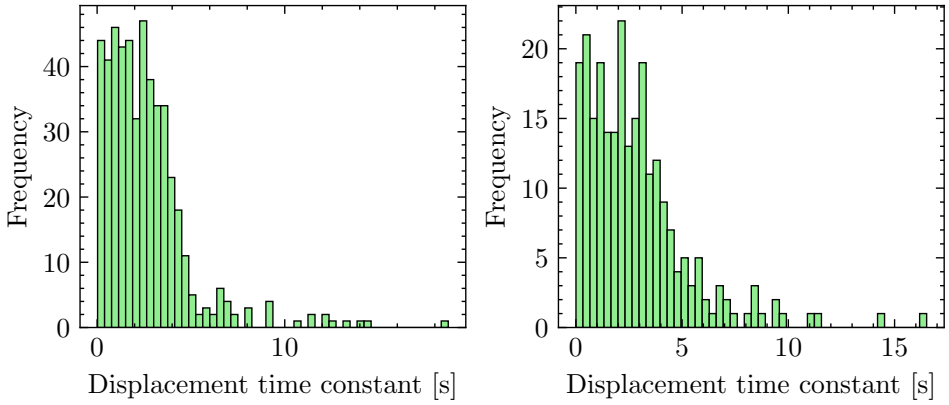

(c) Distribution of displacement time-constant τ in XY(left) and Z(right) DoF [mm]

Figure 4.6: Real displacement data statistical analysis

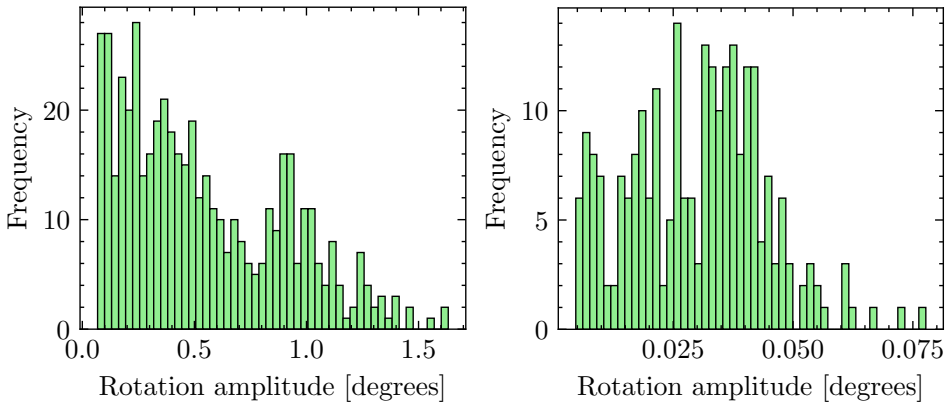

(a) Distribution of rotation amplitude θ in XY(left) and Z(right) DoF [mm]

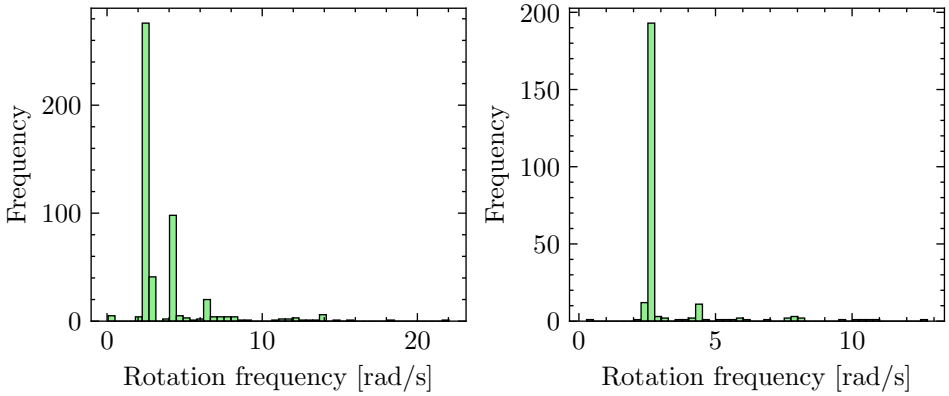

(b) Distribution of rotation frequency ω in XY(left) and Z(right) DoF [mm]

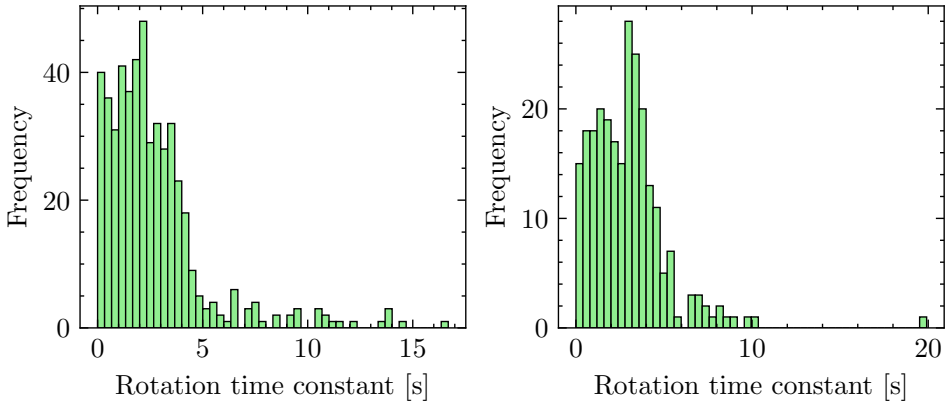

(c) Distribution of rotation time-constant τ in XY(left) and Z(right) DoF [mm]

Figure 4.7: Real rotation data statistical analysis

The statistical analysis shown in figure 4.6 and figure 4.7 was done on 248 vibration sequences with an average length of 10 seconds. The results

for displacement and rotation vibrations are summarised in table 4.3 and table 4.4 respectively. The rotational vibrations have very small amplitude (θ) and is less than 1 degrees for more than 75 percent of the samples in XY plane. For Z axis the vibrations are even smaller with a mean of 0.0005 degrees. These vibrations are very small and do not have a a noticeable visual effect on the video stabilization. But we have decided to account for them to develop a more general solution with multiple applications. The time constant (τ) for displacement and rotation is similar for all DoF with a mean value of around 2.9 seconds. The frequency (ω) for all DoF is also similar in the range $2.5 rad/sec$ to $3.5 rad/sec$. Frequency of $2.5 rad/sec$ is the most dominant frequency and seems to be the natural frequency ω_n of the mechanical system (rig on which the camera is mounted).

The amplitude (A) of the vibration displacement is the most important characteristic for this work as it is main source of video destabilization. The effect of motion on the quality of video is more pronounced in XY plane as the most pixel shift happens here. In Z axis the mean (μ) of vibrations is 0.113 mm with a standard deviation (σ^2) of 0.07 mm. Even the large vibrations in Z seem to have little effect on visual quality of the video. Vibrations in XY plane have the mean of 1.9 mm with a standard deviation of 1.36 mm. Vibrations with higher magnitude are also present and need to be accounted for when generating simulated data.

Parameter	Mean (μ)	Variance (σ^2)	Standard Deviation (σ)
A_{xy}	$1.8944 mm$	$1.8674 mm^2$	$1.3665 mm$
A_z	$0.1135 mm$	$0.0047 mm^2$	$0.0690 mm$
ω_{xy}	$3.6898 rad/s$	$5.9833 rad^2/s^2$	$2.4460 rad/s$
ω_z	$2.6835 rad/s$	$2.0765 rad^2/s^2$	$1.0375 rad/s$
τ_{xy}	$2.5914 s$	$5.1898 s^2$	$2.2781 s$
τ_z	$2.8396 s$	$5.8720 s^2$	$2.4243 s$

Table 4.3: Real Data displacement-vibration distributions

Parameter	Mean (μ)	Variance (σ^2)	Standard Deviation (σ)
θ_{xy}	$0.0094rad$	$3.8729e^{-8}rad^2$	$0.0062rad$
θ_z	$0.0005rad$	$6.0739e^{-8}rad^2$	$0.0002rad$
ω_{xy}	$3.8042rad/s$	$6.3685rad^2/s^2$	$2.5236rad/s$
ω_z	$3.1763rad/s$	$2.6238rad^2/s^2$	$1.6198rad/s$
τ_{xy}	$2.6581s$	$5.8362s^2$	$2.4158s$
τ_z	$2.9316s$	$4.7336s^2$	$2.1757s$

Table 4.4: Real Data rotational-vibration distributions

4.1.2 Simulated Data Generation

The simulated data plays a very important role in our approach as we use the ideal data to validate our stabilization approach. It also empowers us to simulate IMU sensors with different noise levels and characteristics. We also made sure that the data generated from the simulation is fairly domain randomized to make it realistic.

Simulated data is based on the analysed real data with vibration characteristics taken from table 4.3 and table 4.4. The data is then generated using the equations 4.1 and 4.2 .The simulated data is then augmented with modified noise and bias characteristics from table 4.2. A total of 600 vibration sequences with an average vibration duration of 15 seconds was generated with characteristics shown in tables 4.3 and 4.4. Generating a large number of samples ensures the sampling of diverse data from the distribution. This is where we benefit from our simulation the most as the diversity and the size of data ensures our neural network generalizes well.

4.2 Structuring of Data

In classical pose-estimation techniques, every single IMU sample is used individually along with initial condition. Data driven approaches differ in this case as discussed in section 3.2. For data driven approaches instead of taking an individual sample a *window* of samples (figure 4.8)is used as a single sample does not contain enough information. Neural Networks unlike classical mathematics based approaches are data hungry and look for patterns in data and based on these patterns they generate an output. Initially we experimented with small window samples (3 - 20 samples) as shown in figure 4.8 a. This did not yield very good results and the pose estimation error was higher than the required. It started giving good results

once we reach a IMU **window size** of 70 to 140 samples (figure 4.8). Beyond these the performance does not improve much and the inferences from the neural network become computationally expensive and inference latency become very high.

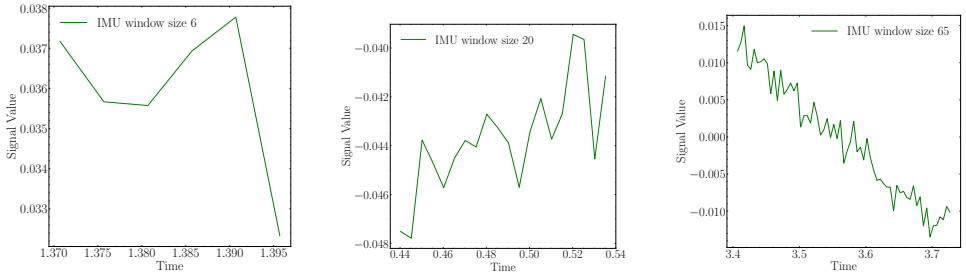

(a) Window size 6, 20 and 65

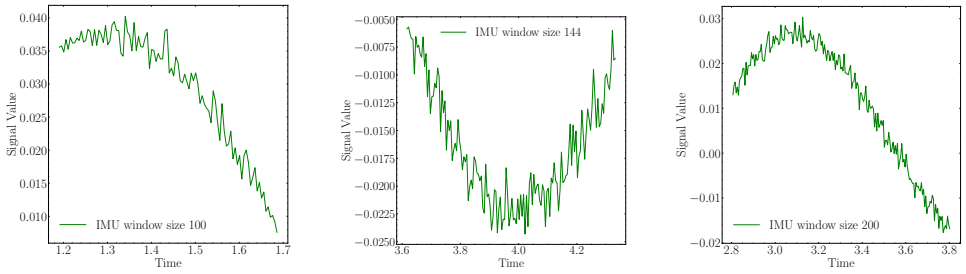

(b) Window size 100, 144, 200

Figure 4.8: Different IMU window samples

4.3 Training and Testing of Various Neural Networks

Various neural networks architectures were trained and tested to accurately estimate the camera pose with respect to a stabilized trajectory. Network takes as input the sensor readings coming from an IMU and the network is trained against the deviation with respect to stabilization trajectory. The stabilization trajectory can be realised as a mean of the vibration displacement (linear/angular) for an ideal case as shown in figure 4.9.

The size of input to the network is variable based on which if we want to only use Accelerometer readings (3, window-size) or both Accelerometer and Gyroscope sensor readings (6, window-size). The use of accelerometer readings is must because destabilization caused in our use case is mostly due to linear displacements as discussed in chapter section 2.3 of this report.

Various neural network architectures like CNN, MLP, LSTM, ResNet, Transformers and their variations were trained and tested for stabilization

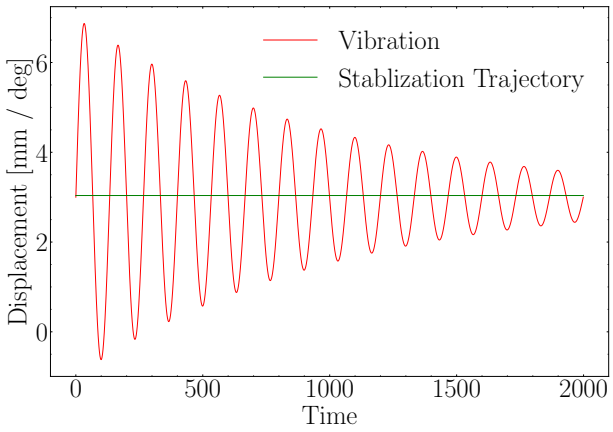

Figure 4.9: Stabilization Trajectory (Ideal)

trajectory regression. Out of these CNN, ResNet and Transformer architectures had acceptable performance.

Note: In the next sections I will be only showing neural network outputs plots for translation as the rotation is very small and all the networks correctly predict it with average error in micro-radians range.

4.3.1 Convolutional Neural Network

Convolution neural network with six **1D-Convolutional** Layers in sequence with **Batch Normalisation** and **ReLU** activation is used to extract features from the input data. Then the output of these convolution layers is regularized using **dropout** and down-sampled using **Max-pooling**. Finally, pose is regressed using a series of two fully connected **Linear** layers.

Model Output Analysis

Figure 4.11 shows the model output vs ground truth plot for a 27 seconds video three linear DoF (x, y, z). The model can regress stabilization trajectory based on input IMU readings with good precision but there are zones where the prediction is off and thus causes jitter in stabilization. The error in all DoF can be seen in figure 4.12.

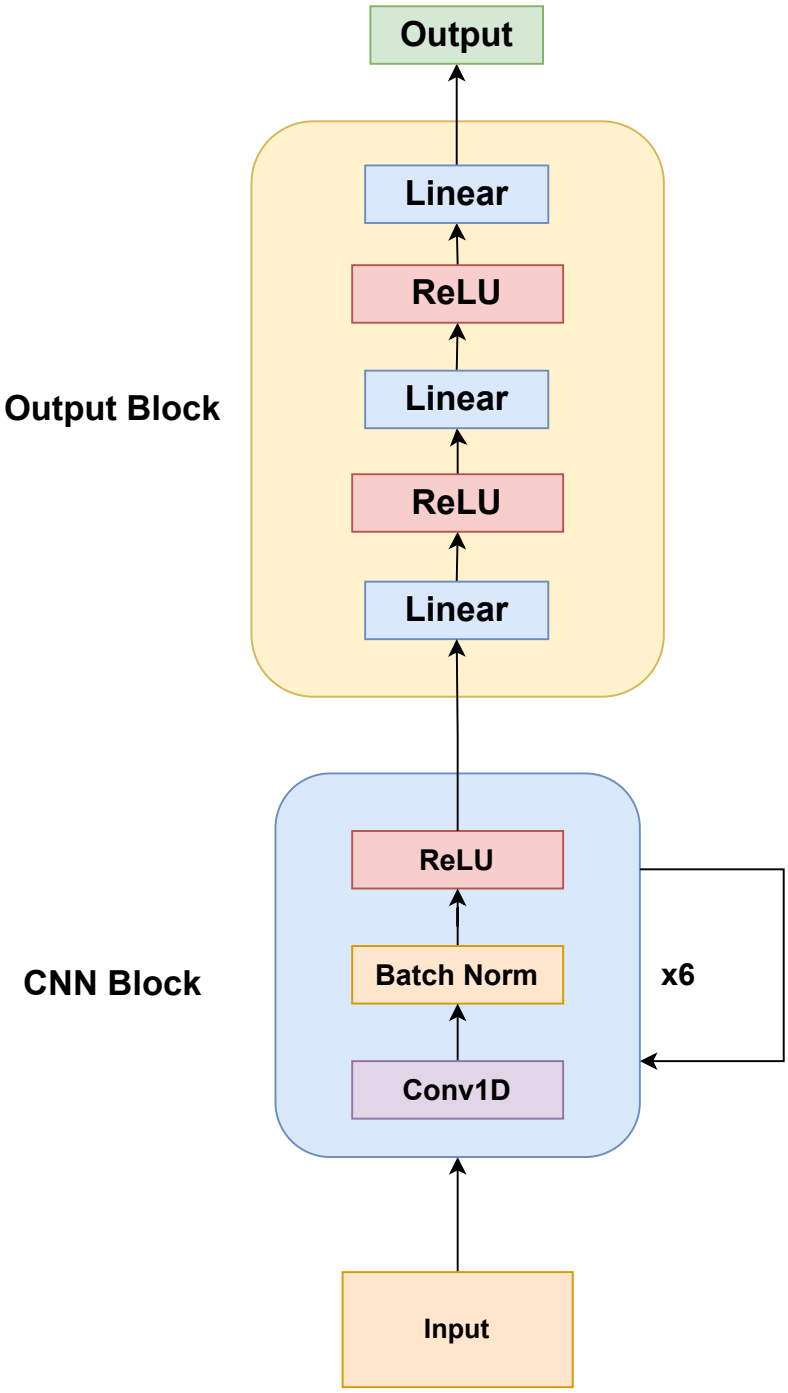

Figure 4.10: Convolutional Neural Network Used

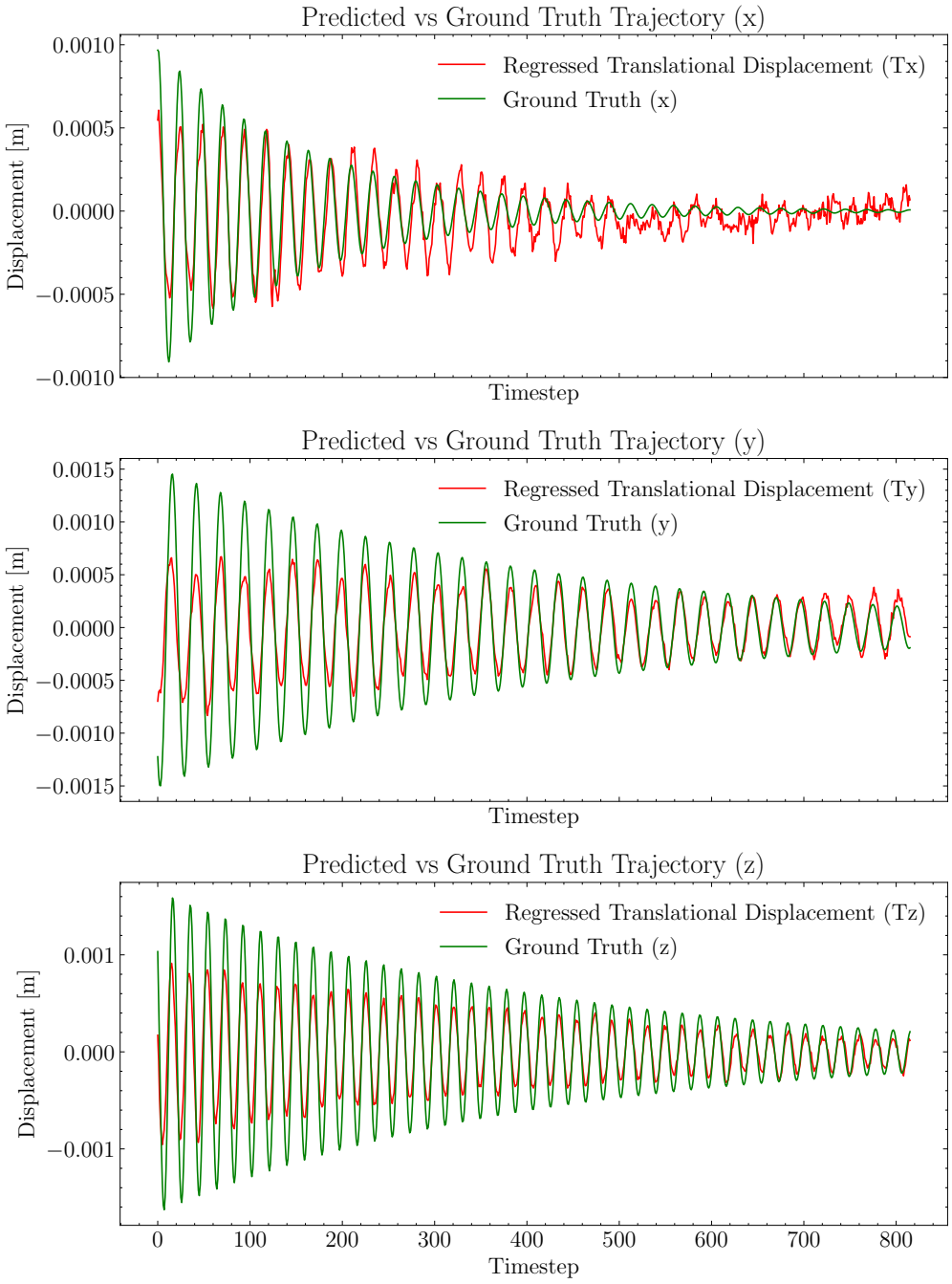

Figure 4.11: Model Prediction vs Ground Truth for CNN

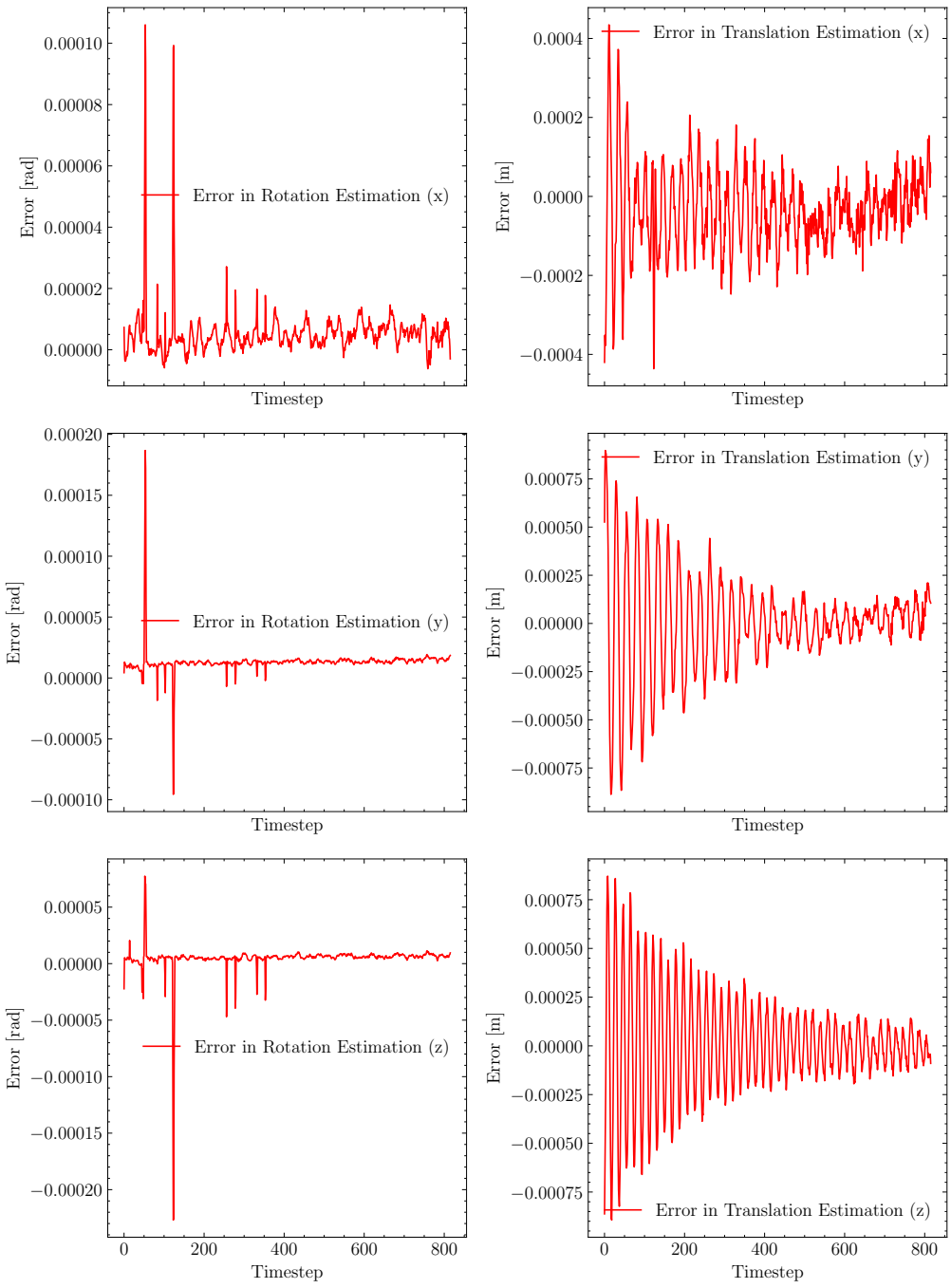

Figure 4.12: Error in each DoF for CNN

4.3.2 ResNet

Convolution neural network having **Residual Skip Connections** with six **1D-Convolutional** Layers in sequence with **Batch Normalisation** and

ReLU activation is used to extract features from the input data. Then the output of these convolution layers is regularized using **dropout** and down-sampled using **Max-pooling**. Finally, pose is regressed using a series of two fully connected **Linear** layers.

Model Output Analysis

Figure 4.14 shows the model output vs ground truth plot for a 27 seconds video three linear DoF (x, y, z). The model can regress stabilization trajectory based on input IMU readings with good precision but there are zones where the prediction is off and thus causes jitter in stabilization. The error in all DoF can be seen in figure 4.15.

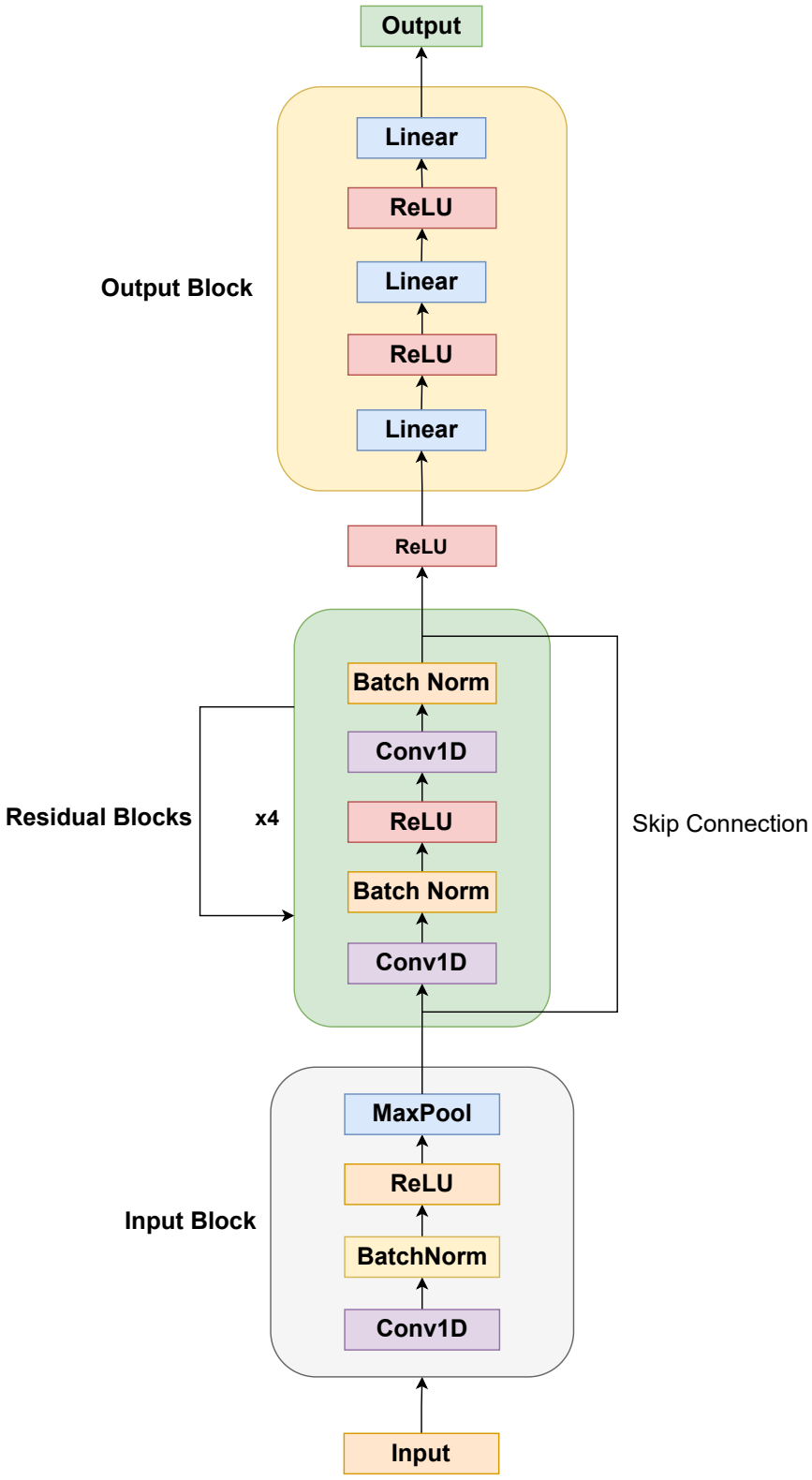

Figure 4.13: CNN with Residual Skip Connections

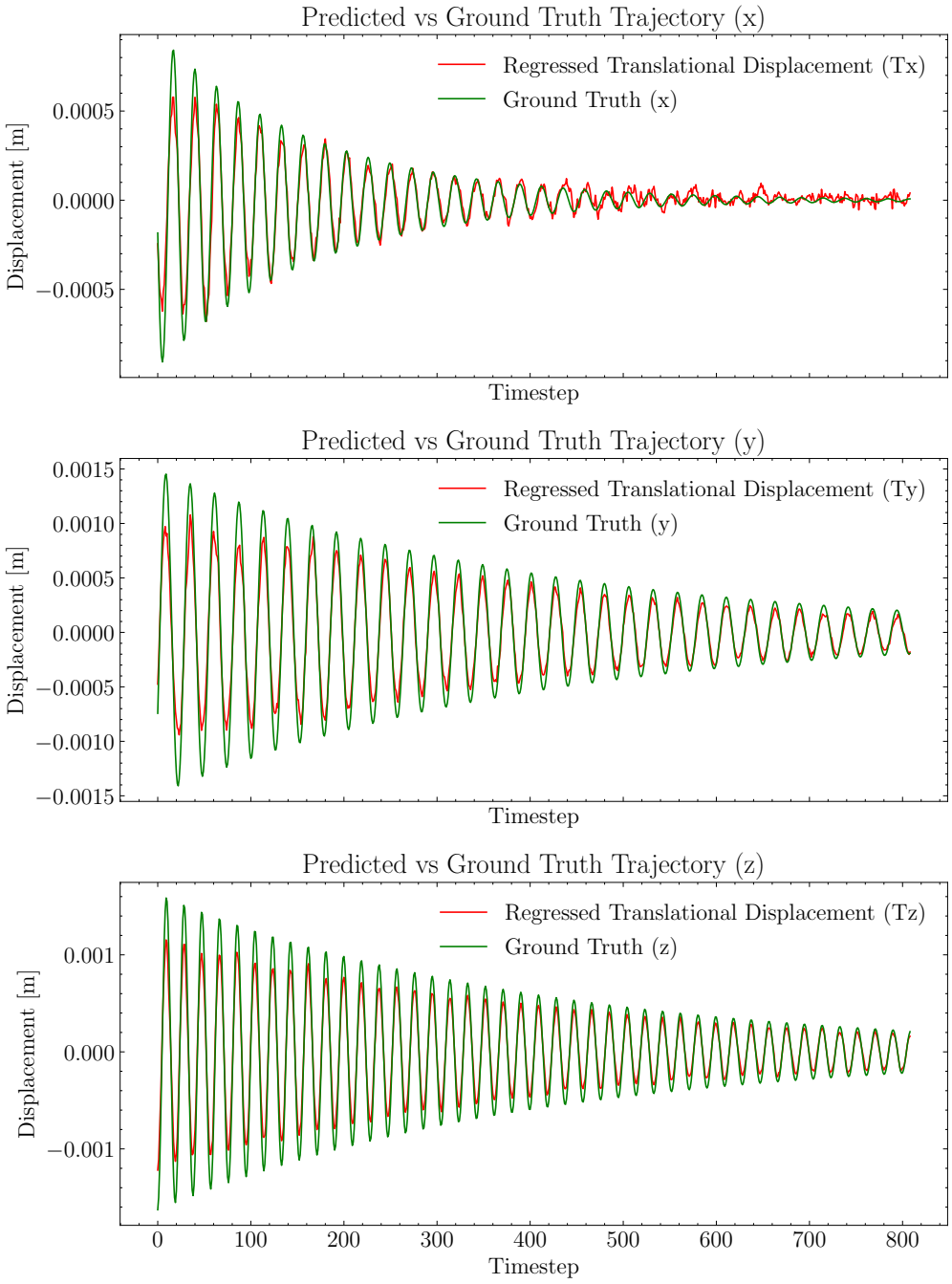

Figure 4.14: Model Prediction vs Ground Truth for ResNet

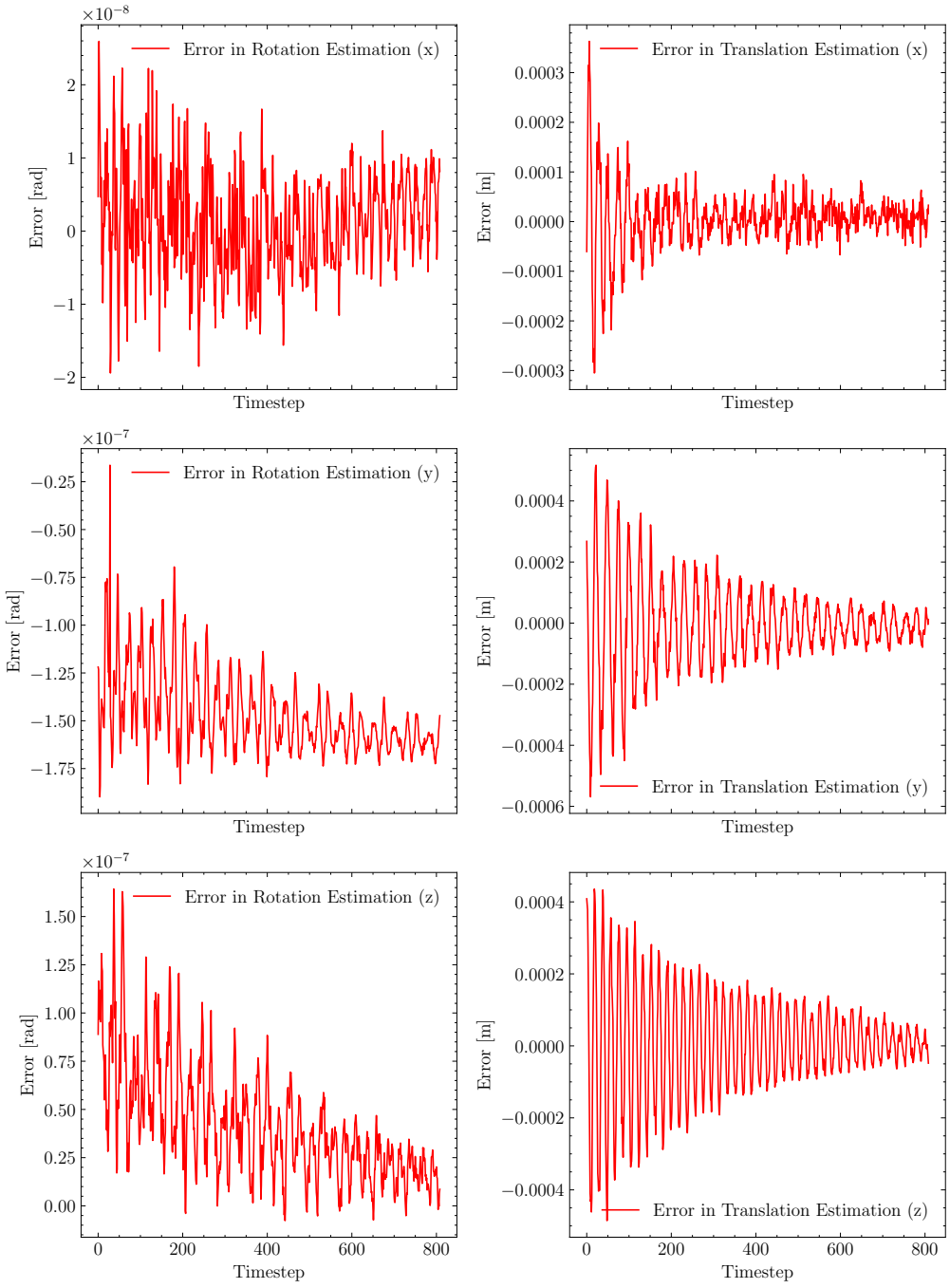

Figure 4.15: Error in each DoF for ResNet

4.3.3 CNN-Transformer

The network is structured in a way that the input goes through four **1D-Convolutional Layers** in sequence with **GELU** activation (non-linear).

The output from these convolutional layers is fed to the *Transformer Encoder*. Transformer Encoder has six layers with each layer having **Multi Headed Attention**, **Dropout**, **GELU** and **Layer Norm**. The output from the encoder layer goes into the output layers consisting of **Layer Normalization**, **Linear** layer, **GELU** non-linearity, **Dropout** and finally a **Fully Connected** layer to regress the output pose.

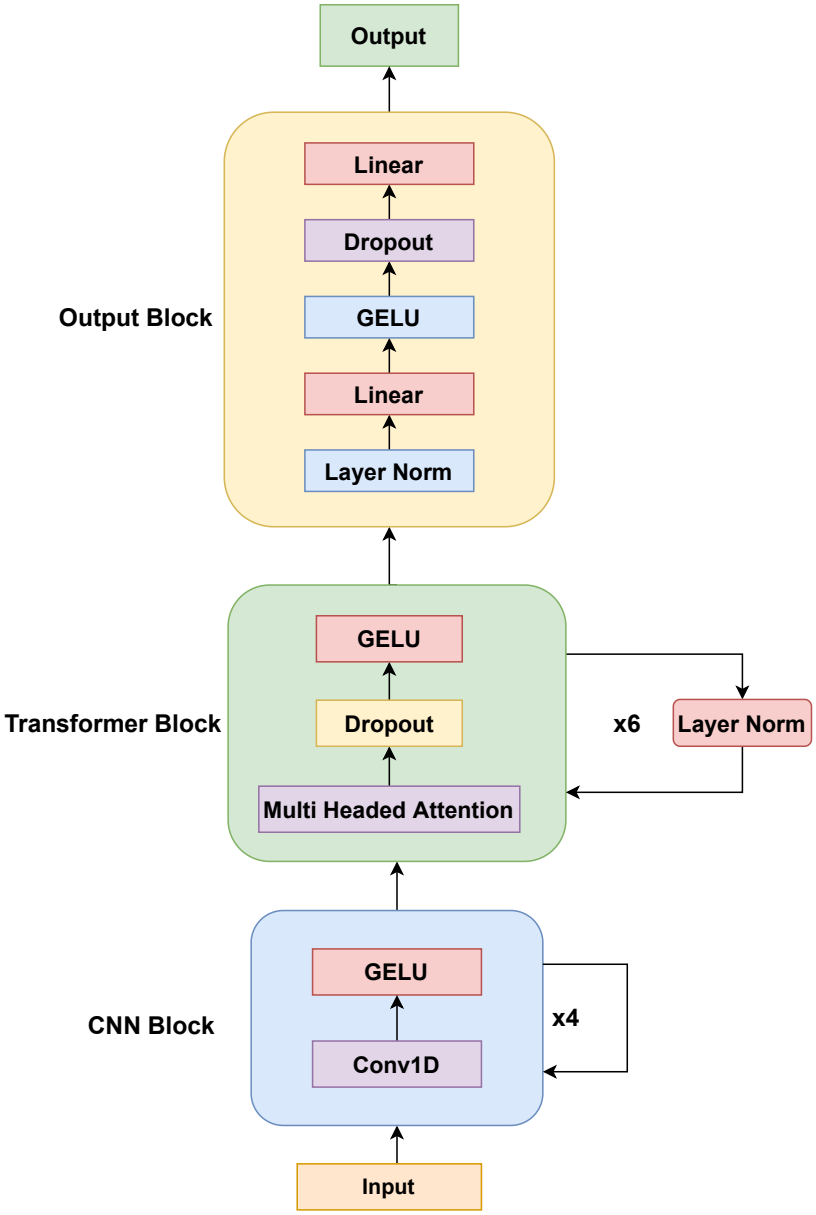

Figure 4.16: CNN-Transformer Network Used

Model Output Analysis

Figure 4.17 shows the model output vs ground truth plot for a 27 seconds video three linear DoF (x, y, z). The model can regress stabilization trajectory based on input IMU readings with very precision and the error is in a very low range of the order of micrometers (μm) and micro radians ($\mu\theta$).

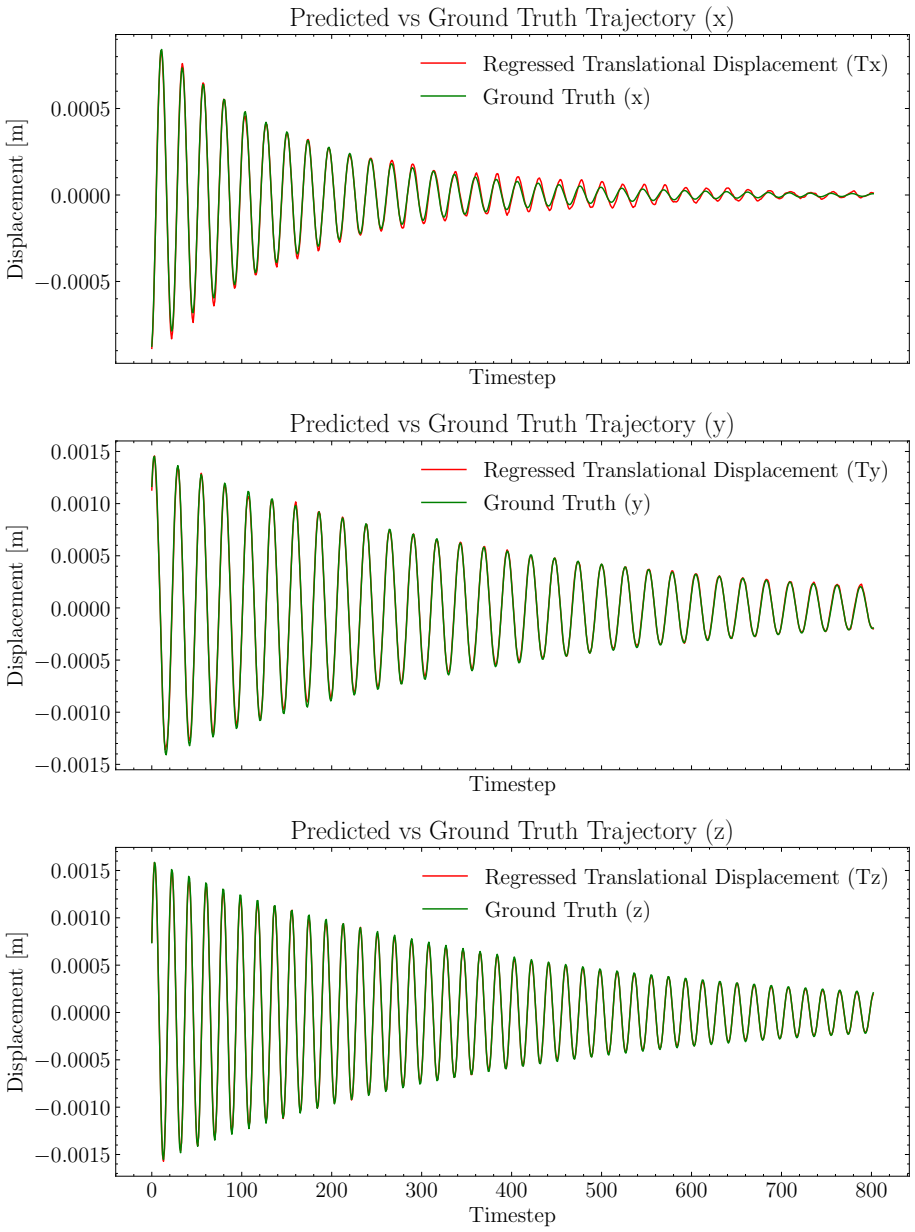

Figure 4.17: Model Prediction vs Ground Truth for CNN-Transformer

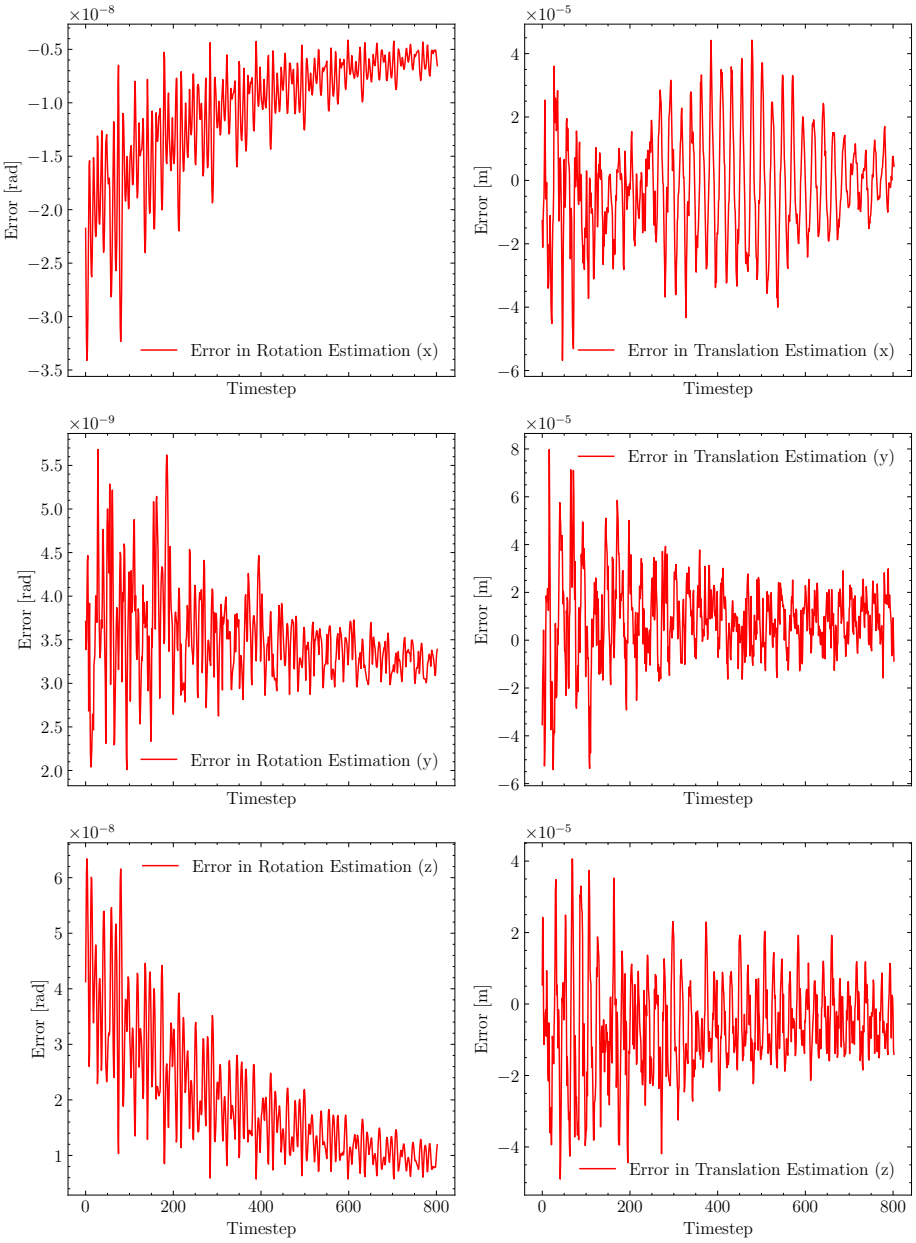

Figure 4.18: Error in each DoF for CNN-Transformer Predictions

4.3.4 Smoothening of Stabilization Trajectory

The neural network is able to regress the stabilization trajectory accurately with the required precision. But the regressed trajectory is not smooth as show in figure 4.19 and has sharp peaks and sudden changes. This is not acceptable as these rough peaks cause jitter in the stabilized video. To account for this, we implemented *Trajectory-Smoothening* in our digital image

stabilization pipeline as shown in figure 4.21. An **Exponential Moving Average Filter** (Equation 4.3) is implemented to smoothen the trajectory and minimise jitter. Figure 4.20 shows the effect of this filter on the model output.

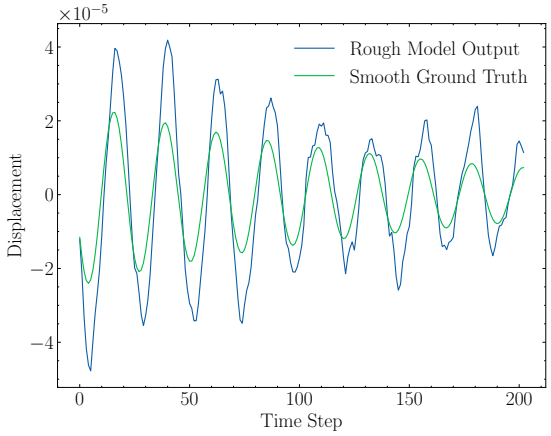

Figure 4.19: Rough regressed vs smooth ground-truth trajectory

$$[H]y_t = x_t \frac{S}{1+H_l} + y_{t-1}(1 - \frac{S}{1+H_l}) \tag{4.3}$$

Where y_t is the smoothened signal and y_{t-1} is the smoothened signal at previous time-step. x_t is the signal value at current time-step. S is the smoothening factor and H is the horizon length. We need to be careful with smoothening the stabilization trajectory because the more we smoothen the higher will be the error introduced in the stabilization trajectory.

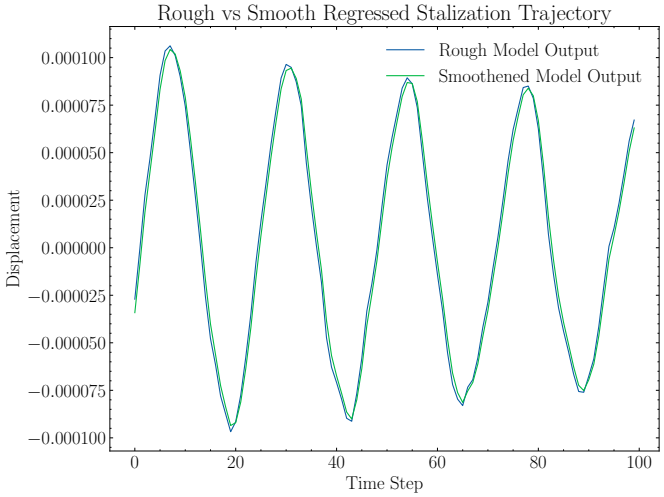

Figure 4.20: Smoothened model output vs raw model output

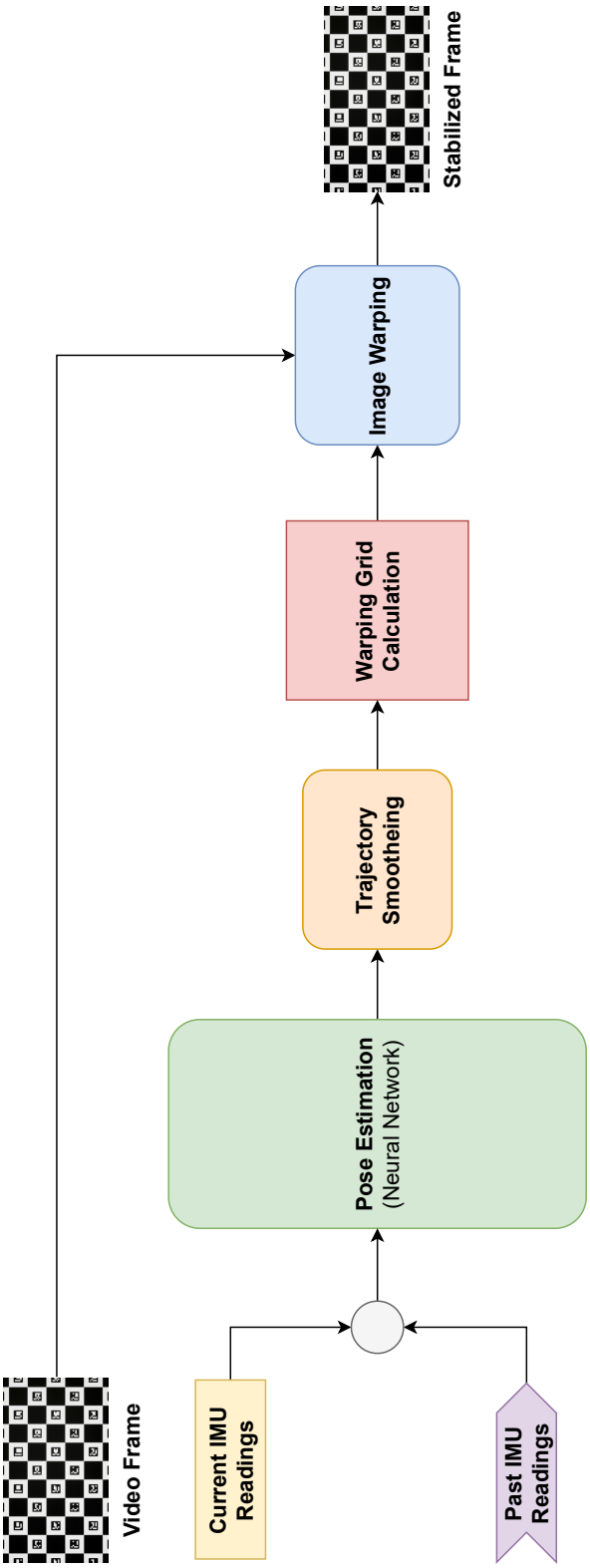

Figure 4.21: DIS Pipeline with Trajectory Smoothening

4.4 Warping Grid Estimation

In our *Digital Image Stabilization Pipeline* (figure 4.1) after getting the relative pose from stabilization trajectory, we need to estimate the warping grid. This warping grid is applied to the image coming from the camera with a crop-ratio of 95 percent (5 percent of the image area will be cropped). These series of warped images based on the pose estimated results into the output stabilized video.

For warping grid calculation we need to estimate *homography* between stabilized trajectory frame (no actual frame in our case because our prediction is always relative to the stabilized trajectory itself) and the current frame. We assume two image points $\boldsymbol{x}$ at times t_i (equation 4.4) and t_j (equation 4.5) from scene points $\mathbf{X}$ as shown in figure 4.22.

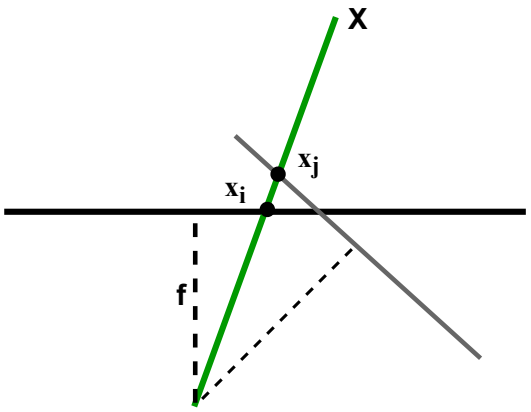

Figure 4.22: Scene points at different time-steps

$$\lambda_i x_i = K(R(t_i)X + p(t_i)) \tag{4.4}$$

$$\lambda_i x_j = K(R(t_j)X + p(t_j)) \tag{4.5}$$

Where, R is the camera rotation, p is the camera position and K is the camera projection matrix (3D to 2D). In our case we have both translation and rotation (although very small). To warp, we need to transform points from camera i to camera j.

$$\lambda_i x_j = KR(t_j)R(t_i)^T \lambda_i K^{-1} x_i - K(R(t_j)R(t_i)^T p(t_i) + p(t_j)) \tag{4.6}$$

$$\lambda_i x_j = K(R_{rel}\lambda_i K^{-1} x_i + p_{rel}) \tag{4.7}$$

The relative rotations and translations between two frames (i and j) are estimated using equations 4.8 and 4.9. These are the values (R_{ij} and t_{ij}) neural networks were trained to predict.

$$R_{ij} = R_i R_i^T \tag{4.8}$$

$$t_{ij} = t_i - R_{ij} t_j \tag{4.9}$$

4.5 Model Deployment

Figure 4.21 shows the digital image stabilization pipeline and our goal is to minimise the time taken at each step. The video (images) are coming at 60 FPS from the camera have 4K resolution (3840x2160 pixels). We ideally have 1/60 seconds (16.67 ms) to complete all the steps of the DIS pipeline. In this pipeline, Model Inference and Stabilization grid calculation take most of the given time. Stabilization grid calculation is a series of matrix multiplications and has been already optimized. Thus, low inference latency is highly desirable.

4.5.1 Making Models Fast

There are many techniques to reduce the inference latency of neural network models. Using these methods may reduce the performance of a neural network but are essential for deployment as models in their original form may not be usable at all. Some of the popular methods are discussed below.

Altering Model Weights

This is a very common approach used to to tackle high latency of deep learning models especially in case of edge hardware deployment. We can **quantize** the model by by converting the weights from floating point (32-bits) to integers (8 bits). This decreases the memory requirements significantly while also improving CPU and hardware accelerator latency (Gambone, 2020).

Another recent approach is to convert the model to **half-precision** (16-bit floating point). It acts as a middle ground between FP32 and INT8 and the performance trade-off is reduced while decreasing the model size. Another very important thing to note is that not all layers have high latency and thus selective weight altering for layers like convolution layers can also be done making the performance trade-off even smaller.

Making Models Lean

The field of deep-learning is growing at a very high rate and we have a large selection of various neural network architectures some even with more than

100 Billion trainable parameters. But while developing deep-learning models, our goal should be to use models with the lowest number of parameters and complex layers while keeping the performance acceptable. The smaller the model is the better its inference latency.

4.5.2 Model Inference Latency on various Hardware

Various trained models (CNN, ResNet and Transformer) are checked for inference latency and the results are summarised in table 4.5. Models were also quantized or converted to ONNX for deployment. The models were inferred 1000 times and the result in the table is an average.

Architecture	Format	No. of Parameters	Inference Latency (ms)
CNN	PyTorch Checkpoint (.ckpt)	00	00
CNN	ONNX (.onnx)	00	00
ResNet	PyTorch Checkpoint (.ckpt)	00	00
ResNet	ONNX (.onnx)	00	00
CNN-Transformer	PyTorch Checkpoint (.ckpt)	00	00
CNN-Transformer	ONNX (.onnx)	00	00

Table 4.5: Inference Latency of Models

This chapter contained all the steps we took and the techniques we used to successfully realise image invariant digital image stabilization using IMU sensor. We examined various neural network architectures for pose-estimation and as expected more modern architectures outperformed the older neural network architectures. Importance of processing neural network outputs to further improve stabilization was also discussed.

4.6 Results and Discussion

This section includes a brief overview of everything we have done and the results we have achieved.

- We have a camera with small FOV high focal length lens which keeps vibrating on its rig after the rig is moved around the scene.
- Vibrations are very small with a mean amplitude of 1.8mm but cause huge pixel shifts in the video recordings thus deteriorating the quality.
- Our goal is to stabilize the video so that there is no visual discomfort for the viewer and quality of the scene is preserved.
- Digital Image stabilization was chosen to stabilize the video for our use case as hardware stabilization is expensive and bulky with a lot of moving parts.
- Camera motion estimation was achieved using MEMS IMU sensor due its low price and high reliability.
- Use of MEMS IMUs present a huge challenge in accurate pose estimation as the noise characteristics of IMU along with the use of classical inertial navigation algorithm makes it impossible to accurately estimate pose accurately. Even the use of advanced state estimation algorithms is futile.
- Both real world and simulated data was collected to train the neural networks and test the image stabilization algorithm.
- Data-driven approaches like RoNIN(CNN and ResNet) were tested to estimate camera pose accurately and showed promising results over classical approaches.
- More advanced self-attention based neural network architectures were used (CNN-Transformer) which improved the accuracy of stabilization trajectory estimation to a very high level.
- This resulted into very good IMU based digital image stabilization.
- Outputs from the neural networks were not smooth causing some jitter in the stabilized video.
- Exponential moving average filter was used on neural network outputs to smoothen the predicted trajectory and improve the quality of video stabilization even more.

4.6.1 Future Work

- Adapt this stabilization technique to high field of view and low focal length camera setups.
- Explore lean neural network architectures to obtain similar results with low latency networks that are deploy-able on cheaper hardware.

- Figure out way to use semi-supervised or unsupervised learning techniques to eliminate the hassle of ground truth generation.

Bibliography

Ahmad, N., Ghazilla, R. A. R., Khairi, N. M., and Kasi, V. (2013). Reviews on various inertial measurement unit (imu) sensor applications. *International Journal of Signal Processing Systems*, 1(2):256–262.

Alatise, M. B. and Hancke, G. P. (2017). Pose estimation of a mobile robot based on fusion of imu data and vision data using an extended kalman filter. *Sensors*, 17(10):2164.

Bangera, S. S., Shiyana, T., Srinidhi, G., Vasani, Y. R., and Sukesh Rao, M. (2020). Mems-based imu for pose estimation. In *Advances in Communication, Signal Processing, VLSI, and Embedded Systems*, pages 1–14. Springer.

Battiato, S., Gallo, G., Puglisi, G., and Scellato, S. (2007). Sift features tracking for video stabilization. In *14th international conference on image analysis and processing (ICIAP 2007)*, pages 825–830. IEEE.

Censi, A., Fusiello, A., and Roberto, V. (1999). Image stabilization by features tracking. In *Proceedings 10th International Conference on Image Analysis and Processing*, pages 665–667. IEEE.

Constant, N., Cay, G., Ravichandran, V., Diouf, R., Akbar, U., and Mankodiya, K. (2021). Data analytics for wearable iot-based telemedicine. In *Wearable Sensors*, pages 357–378. Elsevier.

Cybenko, G. (1989). Approximation by superpositions of a sigmoidal function. *Mathematics of control, signals and systems*, 2(4):303–314.

Dosovitskiy, A., Beyer, L., Kolesnikov, A., Weissenborn, D., Zhai, X., Unterthiner, T., Dehghani, M., Minderer, M., Heigold, G., Gelly, S., et al. (2020). An image is worth 16x16 words: Transformers for image recognition at scale. *arXiv preprint arXiv:2010.11929*.

Ferdinando, H., Khoswanto, H., and Purwanto, D. (2012). Embedded kalman filter for inertial measurement unit (imu) on the atmega8535. In *2012 International Symposium on Innovations in Intelligent Systems and Applications*, pages 1–5. IEEE.

Gambone, R. (2020). Practical Ways to Speed Up your Deep Learning Model. *Xmart Labs Blog*.

Gibson, J. J. (1977). On the analysis of change in the optic array. *Scandinavian Journal of Psychology*.

Grundmann, M., Kwatra, V., and Essa, I. (2011). Auto-directed video stabilization with robust l1 optimal camera paths. In *CVPR 2011*, pages 225–232.

Guilluy, W., Oudre, L., and Beghdadi, A. (2021). Video stabilization: Overview, challenges and perspectives. *Signal Processing: Image Communication*, 90:116015.

Herath, S., Yan, H., and Furukawa, Y. (2020). Ronin: Robust neural inertial navigation in the wild: Benchmark, evaluations, & new methods. In *2020 IEEE International Conference on Robotics and Automation (ICRA)*, pages 3146–3152. IEEE.

Hol, J. D., Dijkstra, F., Luinge, H., and Schon, T. B. (2009). Tightly coupled uwb/imu pose estimation. In *2009 IEEE international conference on ultra-wideband*, pages 688–692. IEEE.

Horn, B. K. and Schunck, B. G. (1981). Determining optical flow. *Artificial intelligence*, 17(1-3):185–203.

Jia, C. and Evans, B. L. (2012). Probabilistic 3-d motion estimation for rolling shutter video rectification from visual and inertial measurements. In *2012 IEEE 14th International Workshop on Multimedia Signal Processing (MMSP)*, pages 203–208. IEEE.

Kok, M., Hol, J. D., and Schön, T. B. (2017). Using inertial sensors for position and orientation estimation. *arXiv preprint arXiv:1704.06053*.

O'Shea, K. and Nash, R. (2015). An introduction to convolutional neural networks. *arXiv preprint arXiv:1511.08458*.

Rao, B., Kazemi, E., Ding, Y., Shila, D. M., Tucker, F. M., and Wang, L. (2022). Ctin: Robust contextual transformer network for inertial navigation. In *Proceedings of the AAAI Conference on Artificial Intelligence*, volume 36, pages 5413–5421.

Ryu, Y. G. and Chung, M. J. (2012). Robust online digital image stabilization based on point-feature trajectory without accumulative global motion estimation. *IEEE Signal Processing Letters*, 19(4):223–226.

Shavit, Y. and Klein, I. (2021). Boosting inertial-based human activity recognition with transformers. *IEEE Access*, 9:53540–53547.

Shi, Z., Shi, F., Lai, W.-S., Liang, C.-K., and Liang, Y. (2022). Deep online fused video stabilization. In *Proceedings of the IEEE/CVF Winter Conference on Applications of Computer Vision*, pages 1250–1258.

Tomasi, C. and Kanade, T. (1991). Detection and tracking of point. *Int J Comput Vis*, 9:137–154.

Trawny, N. and Roumeliotis, S. I. (2005). Indirect kalman filter for 3d attitude estimation. *University of Minnesota, Dept. of Comp. Sci. & Eng., Tech. Rep*, 2:2005.

Vaswani, A., Shazeer, N., Parmar, N., Uszkoreit, J., Jones, L., Gomez, A. N., Kaiser, Ł., and Polosukhin, I. (2017). Attention is all you need. *Advances in neural information processing systems*, 30.

Woodman, O. J. (2007). An introduction to inertial navigation. Technical report, University of Cambridge, Computer Laboratory.

Yan, H., Shan, Q., and Furukawa, Y. (2018). Ridi: Robust imu double integration. In *Proceedings of the European Conference on Computer Vision (ECCV)*, pages 621–636.

Zheng, X., Cui, S., Wang, G., and Li, J. (2015). Video stabilization system based on speeded-up robust features. In *2015 International Industrial Informatics and Computer Engineering Conference*, pages 1995–1998. Atlantis Press.

Zhuang, B., Bai, D., and Lee, J. (2019). 5d video stabilization through sensor vision fusion. In *2019 IEEE International Conference on Image Processing (ICIP)*, pages 4340–4344. IEEE.

Appendix A

First Appendix Chapter

A.1 First Appendix Section

A.1.1 First Appendix Subsection

First Appendix Subsubsection

Declaration of Authorship

I hereby declare that I have written the above Master thesis report independently and that I have not used any sources or aids other than those indicated.

Jena, Germany _____ _____

Ibad Rather